

***Drosulfakinin* signaling encodes early-life memory for adaptive social plasticity**

Jiwon Jeong^{1,8}, Kujin Kwon^{2,8}, Terezia Klaudia Geisseova¹, Jongbin Lee³, Taejoon Kwon^{2,4,5,*}, and Chunghun Lim^{3,6,7,*}

¹ Department of Biological Sciences, Ulsan National Institute of Science and Technology, Ulsan 44919, Republic of Korea

² Department of Biomedical Engineering, Ulsan National Institute of Science and Technology, Ulsan 44919, Republic of Korea

³ Research Center for Cellular Identity, Korea Advanced Institute of Science and Technology, Daejeon 34141, Republic of Korea,

⁴ Center for Genomic Integrity, Institute for Basic Science, Ulsan 44919, Republic of Korea.

⁵ Graduate School of Health Science and Technology, Ulsan National Institute of Science and Technology, Ulsan 44919, Republic of Korea

⁶ Department of Biological Sciences, Korea Advanced Institute of Science and Technology, Daejeon 34141, Republic of Korea

⁷ Graduate School of Stem Cell and Regenerative Biology, Korea Advanced Institute of Science and Technology, Daejeon 34141, Republic of Korea

⁸ These authors contributed equally

*Correspondence: tkwon@unist.ac.kr (T.K.), clim@kaist.ac.kr (C.L.)

Keywords: *Drosophila*; social network behavior; early-life experience; social memory; *Drosulfakinin*.

Abstract

Drosophila establishes social clusters in groups, yet the underlying principles remain poorly understood. Here we performed a systemic analysis of social network behavior (SNB) that quantifies individual social distance (SD) in a group over time. The SNB assessment in 175 inbred strains from the *Drosophila* Genetics Reference Panel showed a tight association of short SD with long developmental time, low food intake, and hypoactivity. The developmental inferiority in short-SD individuals was compensated by their group culturing. By contrast, developmental isolation silenced the beneficial effects of social interactions in adults and blunted the plasticity of SNB under physiological challenges. Transcriptome analyses revealed genetic diversity for SD traits, whereas social isolation reprogrammed select genetic pathways, regardless of SD phenotypes. In particular, social deprivation suppressed the expression of the

neuropeptide Drosulfakinin (*Dsk*) in three pairs of adult brain neurons. Male-specific DSK signaling to Cholecystokinin-like receptor 17D1 mediated the SNB plasticity. In fact, transgenic manipulations of the DSK neuron activity were sufficient to imitate the state of social experience. Given the functional conservation of mammalian *Dsk* homologs, we propose that animals may have evolved a dedicated neural mechanism to encode early-life experience and transform group properties adaptively.

Introduction

Animals interact with other individuals in distinct social environments (1-3). For instance, a pair of animals display aggression or mating behaviors, whereas a group of individuals may show collective behaviors through intricate networks of social interactions. Such social network behaviors (SNB) are believed to enhance group fitness and are conserved across many species, underscoring their evolutionary significance (3, 4). Additionally, social interactions influence various physiological activities in individuals, including feeding, sleep/circadian rhythms, aggression, stress response, and longevity (5-11). Nonetheless, it remains elusive how group properties have evolved with other individual traits and how animals process social experiences to shape their behavior and physiology.

Drosophila has long been considered a solitary species. Yet a group of flies can display distinct SNB under specific experimental conditions (12-17), serving as an ideal genetic model to address our questions above (2). Previous studies have employed various biophysical parameters to quantify both individual and network behaviors in groups, establishing criteria for social interactions in *Drosophila* (2, 13, 14, 18). While these measurements give a comprehensive view of group behaviors, our study focuses on the clustering property of social interactions within a group (13, 19). Social clustering is an intuitive measure that integrates diverse social interactions via multiple sensory cues (12, 13, 18, 19), accompanying reductions in social distance (SD) among group members and their moving speed over time. We also reasoned that simple SD assessment could facilitate the alignment of large-scale datasets of group behaviors with physiological traits, differential gene expression, and neurogenetic manipulations.

These approaches lead to our demonstration that the group property for high social clustering (i.e., short SD) is closely associated with and compensates for inferior developmental traits in individuals. Moreover, *Drosophila* can adjust their social preferences according to physiological changes, indicating the adaptive plasticity of SNB. This social plasticity requires early-life social experiences that persist throughout development. We also define a specific neuropeptide signaling pathway that encodes social memory and supports SNB plasticity. Our findings thus provide new insights into

the principles of SNB, offering a deeper understanding of the evolutionary and genetic bases of social behaviors in *Drosophila* and possibly other species.

Results

SNB is a quantitative trait in a natural *Drosophila* population

We employed the *Drosophila* Genetic Reference Panel (DGRP) to determine whether SNB has evolved with specific genetic factors and physiology. The DGRP consists of approximately 200 inbred wild-type strains and functions as a practical genetic library to explore the correlation between naturally occurring genetic variations and complex animal behaviors (20-22). We video-recorded a group of 16 male flies freely moving in an open arena for 10 min and quantitatively assessed their group properties over time (Figure 1A). These included SD between individual group members (Figure 1B), walking speed, and the centroid velocity of a given group. The DGRP lines displayed a range of distributions for the three parameters (Figure 1C; Figure 1—source data 1), and we found their significant correlations among 175 DGRP lines (Figure 1D; Figure 1—source data 1; Spearman correlation analysis). For instance, short-SD lines gradually reduced SD and walking speed over time to stay in the cluster, thereby exhibiting short travel distances, slow walking speeds, and low centroid velocities on average (e.g., DGRP73, DGRP 563, and DGRP370) (Figure 2A; Figure 2—figure supplement 1; Figure 2—source data 1; Video 1). By contrast, long-SD lines persistently explored the arena during video recording and sustained “social distancing” to display long travel distances, fast walking speeds, and high centroid velocities (e.g., DGRP360, DGRP707, and DGRP317) (Figure 2B; Figure 2—figure supplement 1; Figure 2—source data 1; Video 2) although their locomotion was modestly slowed down over time. The locomotion trajectories of individual flies confirmed these characteristics (Figure 2C and D; Figure 2—source data 1), and long-SD individuals traveled much longer distances than short-SD individuals across the DGRP lines (Figure 2—figure supplement 1C; Figure 2—source data 1). Short-SD flies did not significantly change their locomotor activity over time when we placed a single fly in the same arena and assessed its behavior (Figure 2—figure supplement 2; Figure 2—source data 1). Thus, reduced activity in a group of short-SD flies is likely an effect of their clustering phenotypes but not necessarily the cause. Short- and long-SD flies retained their clustering properties even in a larger arena (Figure 2—figure supplement 3; Video 3 and 4; 8.5 cm in diameter), indicating active social preferences that persist in different environments. Both types of DGRP lines displayed no chaining behaviors in the open arena, excluding the possible implication of male-to-male courtship in their SD phenotypes (Figure 2—figure supplement 4; Figure 2—source data 1). These results provide convincing evidence that SD is an inheritable group trait from natural *Drosophila* variants. Based on the average ranking of individual DGRP lines in the two group properties (i.e., SD and centroid

velocity), we selected the top and bottom three DGRP lines representing short- and long-SD phenotypes, respectively, to elucidate the physiological significance of *Drosophila* SNB and its underlying mechanisms.

Social interactions compensate for developmental inferiority in short-SD larvae

Why do flies display SNB? One clue comes from the previous observation that *Drosophila* larvae collectively dig culture media and improve food accessibility, possibly facilitating their constitutive feeding during early development (15). In fact, we found that the short-SD lines had higher numbers of larvae per cluster than the long-SD lines (Figure 3A; Figure 3—source data 1). These observations suggest that *Drosophila* express SNB traits from early development, and the sociality persists in adults. To better define the social-interaction effects on *Drosophila* physiology, we obtained socially enriched or deprived larvae from fertilized eggs (Figure 3B) and then compared their developmental phenotypes among DGRP lines. Social isolation substantially impaired larval activity and development in both short- and long-SD lines (Figure 3C-G; Figure 3—source data 1). We further found that the short-SD trait is tightly associated with inferior phenotypes, particularly in isolated larvae. For instance, socially isolated larvae from the short-SD lines displayed poor digging activity (Figure 3C; Figure 3—source data 1), low food intake (Figure 3D; Figure 3—source data 1), and long developmental time (Figure 3E; Figure 3—source data 1) compared to those from the long-SD lines. Short-SD larvae also had lower eclosion success (Figure 3F; Figure 3—source data 1) and a lower ratio of the adult male progeny (Figure 3G; Figure 3—source data 1) than long-SD larvae although isolated cultures reduced the eclosion success regardless of the SD trait. Grouping of short-SD larvae blunted or partially rescued these phenotypes (i.e., digging activity, developmental time, eclosion success, and male progeny ratio). Our group culture was not a competitive environment for limited resources to delay developmental time (23, 24), but it actually promoted food intake comparably in short- and long-SD larvae (Figure 3D; Figure 3—source data 1). The significant interaction effects of social distance (i.e., short- vs. long-SD trait) and socialization (i.e., grouped vs. isolated cultures) on digging activity, developmental time, and male progeny ratio suggest that the clustering property of short-SD lines may have evolved as a compensation mechanism for the developmental inferiority in individuals. Considering that a low percentage of male likely limits mating choice, reproductive efficiency, and genetic diversity in a given group, social interactions may also contribute to the group fitness in short-SD lines across generations. We speculate that the feeding amount of isolated long-SD individuals is saturating for normal development (e.g., developmental time, male progeny ratio), possibly explaining the lack of interaction effects on food intake while displaying developmental inferiorities most evidently in isolated short-SD individuals.

Early-life experience is necessary for social benefits on adult physiology and adaptive social plasticity

We further asked whether social interactions also benefit adult physiology in the short-SD lines. To this end, we designed a maze experiment where a group of flies were placed in a novel arena to determine how fast they could reach a food resource in the presence or absence of pre-trained flies (Figure 4A). Our prediction was that social interactions between naïve and trained flies might facilitate their food-seeking, possibly mimicking social foraging in other species (25). We first confirmed that both short- and long-SD lines significantly shortened latency to the arrival of 75% of flies on food by iterative exposures to the maze (Figure 4B; Figure 4—figure supplement 1; Figure 4—source data 1). Representative plasticity mutants of the *rutabaga* (*rut*) gene did not significantly shorten the arrival latency after three consecutive training sessions in our maze paradigm (Figure 4—figure supplement 2A; Figure 4—source data 1), implicating *rut*-dependent learning and memory in this process (26). The short-SD lines displayed poor performance in the maze assay as assessed by longer latency to the arrival of 75% naïve flies on food than the long-SD lines (Figure 4B; Figure 4—figure supplement 1; Figure 4—source data 1). Combining the trained “pioneers” with a group of naïve flies significantly improved the group property of food-seeking behaviors in both short- and long-SD lines (Figure 4B; Figure 4—figure supplement 1; Figure 4—source data 1). The pioneer effects disappeared when the naïve group consisted of socially isolated individuals from egg development. These results support that social foraging in our maze paradigm is unlikely a simple collective response in adults, but it specifically requires early-life social experience. Of note, social deprivation effects on pioneer-free group foraging somewhat varied across the long SD lines (Figure 4B; Figure 4—figure supplement 1; Figure 4—source data 1). We reason that the hyperactivity of individual long-SD flies facilitates their food-seeking behaviors in the maze, weakening the pioneer effects or even overriding the group property.

The long-SD lines outcompeted the short-SD lines in both larval and adult assays, and the beneficial effects of their social experience were barely detectable. SNB in the long-SD adults was also insensitive to early-life experience, whereas the grouped culture promoted SNB in the short-SD lines (18) (Figure 2—figure supplement 1B; Figure 2—source data 1). We hypothesized that superior traits in long-SD individuals led to their genetic selection toward the degeneration of social interaction effects. Alternatively, long-SD genomes may still encode genetic programs for social activity, but they only express social traits under physiologically challenging conditions. Given the positive correlation between locomotion activity and SD trait among DGRP lines (Figure 1D; Figure 1—source data 1), we reasoned that modest injury could serve as a physiological cue to reduce locomotor activity in individuals, facilitate their interactions in a group, and induce SNB even in the long-SD flies. We indeed discovered that mechanical injury shortened SD in both sociality types of DGRP lines (Figure 4C and D;

Figure 4—figure supplement 3A; Figure 4—source data 1; Video 5 and 6;) while reducing walking speed and centroid velocity only in the long-SD lines (Figure 4—figure supplement 4; Figure 4—source data 1). The injury effects were transient because one week of recovery was sufficient to restore the original SD traits (Figure 4D; Figure 4—figure supplement 3A; Figure 4—source data 1). The injury-induced plasticity of SNB and locomotor activity was not detectable in a group of socially isolated flies (Figure 4D; Figure 4—figure supplement 3A, 4; Figure 4—source data 1; Video 7-10). We thus reason that the mechanical injury does not severely impair general locomotion per se to abolish or overestimate SNB under our experimental conditions, but low activity in grouped long-SD flies is likely a consequence of their injury-induced clustering. The injury-induced SNB plasticity required *no receptor potential A (norpA)* among sensory pathway genes tested (Figure 4—figure supplement 5; Figure 4—source data 1), indicating a crucial role of *norpA*-dependent visual sensing. It is consistent with the previous finding that vision is required for larval clustering behaviors in *Drosophila* (15). We further found that an adult-specific grouping of developmentally isolated flies was insufficient to support the social plasticity (Figure 4D; Figure 4—figure supplement 3A; Figure 4—source data 1). Finally, the *rut*-dependent memory pathway seems dispensable for developmental “social memory” since *rut* mutants displayed injury-induced social plasticity comparable to control flies (Figure 4—figure supplement 2B; Figure 4—source data 1). These results suggest that individual *Drosophila* strains differentially display social traits in adults; however, the potency of adaptive social plasticity is acquired through their early-life experience of social interactions.

Unraveling the genetic basis of SNB and its plasticity

How is early-life social experience encoded in individual larvae to persist throughout development? To define the molecular signatures of social interaction phenotypes and their plasticity, we profiled differentially expressed genes (DEGs) in adult fly heads among distinct contexts of genetic and environmental sociality. The transcriptome analyses revealed significantly upregulated genes in the short- and long-SD lines (n genes = 191 and 199, respectively), as well as in grouped and socially isolated flies (n genes = 159 and 755, respectively) (Figure 5A and B; Figure 5—source data 1, 2). Genes upregulated in socially isolated DGRP lines overlapped substantially with those identified in previous studies using independent wild-type strains (8, 27, 28) (Figure 5—figure supplement 1A; Figure 5—source data 3), whereas upregulated genes in short- or long-SD lines barely overlapped with DEGs between grouped and socially isolated flies (Figure 5—figure supplement 1B; Figure 5—source data 3). Gene ontology (GO) analyses showed no significant enrichment of specific GO terms in DEGs between the short- and long-SD lines. We thus concluded that diverse genetic pathways shape baseline SD phenotypes, as suggested previously (12). It is also consistent with the lack of the phylogenetic correlation between *Drosophila* species and their social network

phenotypes (29). By contrast, select metabolic pathways were upregulated in both types of DGRP lines by social isolation (Figure 5C and D; Figure 5—source data 2, 4). These observations were consistent with previous findings that chronic social isolation acts as a hunger cue to suppress sleep, induce feeding, and alter metabolic gene expression, including those involved in lipid metabolism (8, 30). Considering that the number of commonly upregulated genes in group-cultured flies was very limited, we speculate that *Drosophila* has evolved a genetic reprogram where social isolation elevates metabolic gene expression to adaptively induce a metabolic shift for energy storage and fitness.

Interestingly, the phenotypic alignment of DGRP lines revealed significant correlations of their social interaction behaviors to food intake, starvation-induced activity, and aggression, among others (31-33) (Figure 5E; Figure 5—source data 5). We validated that the long-SD lines showed more lunges than the short-SD lines, indicative of high aggression behaviors (Figure 5—figure supplement 2; Figure 5—source data 5; Video 11 and 12). The association of multiple behaviors raised the possibility of their overlapping evolution of regulatory genes and mechanisms. The expression heatmaps of relevant gene categories visualized a subset of genes that indeed displayed social experience-dependent expression across the DGRP lines analyzed (Figure 5F; Figure 5—source data 1). These included *Drosulfakinin* (*Dsk*), a neuropeptide implicated in aggression, food intake, satiety, and sexual behaviors (28, 34-37). The mammalian *Dsk* homolog cholecystokinin (CCK) has also been shown to play a similar role in relevant physiology, suggesting the possible conservation of *Dsk* function (38-40). In fact, *Dsk* was the only overlapping gene that was downregulated upon social isolation across independent studies (8, 27, 28) (Figure 5—figure supplement 1A; Figure 5—source data 3). We also found that social isolation of the DGRP lines significantly downregulated the expression of *Dsk* and the two CCK-like receptors (i.e., *CCKLR-17D1* and *CCKLR-17D3*), although *Dsk* receptor gene expression showed less than two-fold change (Figure 5F; Figure 5—source data 2). These observations prompted us to ask whether DSK signaling contributes to the plasticity of social behaviors through early-life experience.

DSK neuron activity encodes early life experience for SNB plasticity

Immunostaining of whole-mount brains identified three groups of DSK-expressing neurons with distinct neuroanatomical morphology (i.e., MP1a, MP1b, and MP3) (34, 35) (Figure 6A). The long-SD lines displayed relatively high DSK signals in the cell bodies compared to the short-SD lines (Figure 6B; Figure 6—source data 1). However, DSK levels in the neural projections were comparable between the two groups, raising the possibility that axonal transport or processing of the neuropeptide was limiting under the group-culture condition. Social isolation lowered DSK levels irrespective of the SD phenotype (Figure 6A and B; Figure 6—source data 1), consistent with our DEG analysis above. The social experience effects on DSK levels were most evident in the

MP1a neuron projections. Live-brain imaging of the genetically encoded Ca^{2+} indicator GCaMP showed that DSK neuron activity correlated with social experience and plasticity in a wild-type background. Social deprivation reduced relative Ca^{2+} levels in DSK neurons, whereas mechanical injury generally elevated DSK neuron activity (Figure 6C; Figure 6—source data 1). The two conditions, however, acted independently on the GCaMP signals in DSK neurons since their interaction effects were not significantly detected. Nonetheless, MP1a neuron activity did not respond to injury when transgenic flies were socially deprived during development, which may contribute to the lack of social behavior plasticity upon isolation (Figure 6C and Figure 6—figure supplement 1; Figure 6—source data 1). These observations are unlikely due to transgenic *Dsk*-Gal4 activity per se given that social isolation did not comparably affect the Gal4-dependent expression of a dendritic marker transgene in the DSK neurons (Figure 6—figure supplement 1; Figure 6—source data 1). We also confirmed that GCaMP levels in other neuropeptide-expressing neurons (i.e., Pigment-dispersing factor) were insensitive to social isolation or mechanical injury (Figure 6—figure supplement 2; Figure 6—source data 1).

We used the transsynaptic mapping transgene trans-Tango to visualize the postsynaptic partner of DSK neurons via heterologous ligand-receptor signaling (41, 42). Socially enriched, but not socially isolated, male flies displayed strong postsynaptic signals of the trans-Tango-expressing DSK neurons in the lateral protocerebrum where transgenic signals of DSK neuron axons (*Dsk*>SyGFP) were readily detectable (Figure 6D and E; Figure 6—figure supplement 1B; Figure 6—source data 1). Previous studies also demonstrated that MP1a neuron projections are specifically enriched in this brain region (34, 35). DSK neurons have gender-specific presynaptic partners, which may mediate distinct signaling for sexual behaviors (34, 35, 37, 43). To our surprise, socially enriched female brains did not show trans-Tango signals as evidently as male brains (Figure 6D and E; Figure 6—source data 1). Moreover, social deprivation downregulated DSK levels in the MP1a projections less potently in females than in males (Figure 6D and F; Figure 6—source data 1). These observations suggest sexual dimorphism in social behavior plasticity. Indeed, female flies from select DGRP lines showed baseline SD phenotypes consistent with their male counterparts, yet mechanical injury did not significantly affect female SD (Figure 4—figure supplement 3B, Figure 4—source data 1; also see Figure 7G; Figure 7—source data 1). Considering that DSK-expressing MP1 neurons originate from the larval brain (44), we hypothesized that early-life experience is developmentally encoded in DSK neuron activity via the male-specific neural pathway and adaptively expressed for social plasticity in adults. We further reason that low food intake upon social isolation may not directly implicate DSK expression or DSK neuron activity since DSK signaling has been shown to suppress feeding behavior as a satiety cue (35, 36, 45, 46).

Male-specific DSK-CCKLR-17D1 signaling mediates SNB plasticity

To determine whether DSK signaling actually contributes to social behavior plasticity, we first examined the loss-of-function effects of relevant genes. Genomic deletion of the *Dsk* locus (*Dsk*^{attP}) or DSK depletion by RNA interference (*Dsk*>*Dsk*^{RNAi}) abolished injury-induced clustering behaviors (Figure 7A-C; Figure 7—figure supplement 1; Figure 7—source data 1). Furthermore, genomic deletions of the *Dsk* receptor *CCKLR-17D1* (*CCKLR-17D1*^{attP} and *CCKLR-17D1*^Δ) but not *CCKLR-17D3* (*CCKLR-17D3*^{attP} and *CCKLR-17D3*^Δ) comparably masked injury-induced social interactions (Figure 7B; Figure 7—figure supplement 2; Figure 7—source data 1). Genetic effects of *Dsk* deletion and DSK depletion were not consistent on baseline SD in grouped cultures. These observations suggest that *Dsk* is not crucial for shaping the SD traits per se, but genetic backgrounds may substantially contribute to it. Nonetheless, genetic evidence from independent alleles and transgenic RNAi convincingly supports specific implication of the DSK-CCKLR-17D1 pathway in experience-dependent social plasticity.

We further validated if neuronal activity or synaptic transmission for DSK-CCKLR-17D1 signaling controls injury-induced SNB plasticity. To this end, a temperature-sensitive allele of *Drosophila* dynamin (*shibire*^{ts}) (47) was transgenically expressed in DSK neurons to block their synaptic transmission only at restrictive temperature (Figure 7D). The conditional manipulation of larval DSK neurons was sufficient to suppress injury-induced clustering in group-cultured adults (Figure 7E; Figure 7—source data 1). CCKLR-17D1-expressing neurons displayed a gender-specific distribution in the adult brain when their dendrites and axons were visualized using specific transgenic markers (i.e., DenMark and SytGFP, respectively) (Figure 7F). In particular, male brains expressing the CCKLR-17D1 knock-in transgene showed more signals for cell bodies and dendrites around MP1a axon projections than females (35). This was consistent with the high levels of axonal DSK expression and trans-Tango signals in the same region of male brains (Figure 6D-F; Figure 6—source data 1). We hypothesized that transgenic activation of DSK-CCKLR-17D1 signaling genetically mimics social experience in developmentally isolated flies. Supporting this idea, transgenic excitation of CCKLR-17D1 neurons was sufficient to confer injury-induced social interactions to isolated male flies (Figure 7G; Figure 7—source data 1). The same transgenic manipulation of CCKLR-17D1 neurons did not induce social plasticity in females, irrespective of their early-life experience. On the other hand, blocking synaptic transmission in CCKLR-17D1 neurons suppressed injury-induced clustering in group-cultured male flies (Figure 7—figure supplement 3; Figure 7—source data 1). These findings convincingly provide a neuroanatomical basis for early-life social memory and male-specific social plasticity.

Discussion

Our study demonstrated that conspecific individuals show a wide range of preferences for social distancing, and it has likely co-evolved with their inferior traits as a compensatory mechanism (Figure 8). Physiological challenges (e.g., mechanical injury) may adaptively modify the clustering property of a given group. However, the plasticity of group behaviors requires social experience during development. We propose that a subset of the *Drosophila* brain neurons expressing the neuropeptide DSK serves as a neural substrate for social memory, as supported by the intimate coupling of early-life social experience and SNB plasticity to DSK expression, DSK neuron activity, and post-synaptic signaling.

Distinct social behaviors in *Drosophila* (i.e., aggression and mating) have been commonly mapped to specific pairs of DSK neurons (34, 35, 37). Presynaptic partners of DSK neurons are sexually dimorphic, while their post-synaptic effects are differentially mediated via the two DSK receptor pathways (i.e., CCKLR-17D1 for aggression and SNB plasticity; CCKLR-17D3 for sexual behaviors). Intriguingly, this neural architecture for balancing aggression and mating behaviors has been proposed to be analogously conserved between flies and mammals (48). Furthermore, DSK neuron activity correlates with social dominance (i.e., winner effects from aggression) (35) and group housing (34), but not with mating status (37). Accordingly, the DSK-CCKLR-17D1 pathway meets the necessary criteria for male-specific SNB plasticity.

The phenotypic correlates of aggression and SNB in natural populations (i.e., DGRP lines) are consistent with their common neural locus. However, these findings do not necessarily imply that DSK neurons control the two social behaviors in a similar manner. For instance, DSK excitation promotes aggression in both males and females (35), whereas DSK signaling is unlikely to trigger grouping behaviors per se. What remains to be clarified is how DSK signaling gates SNB plasticity and why this process is missing in female flies. Considering that social hierarchy is established in male fights only (49, 50), we speculate that male-specific DSK pathways may include extra circuit modalities for contextual processing of social environments and adaptive social structures. The development of neuroanatomical differences between male and female brains may coincide with the acquisition of gender-specified demands for innate behaviors and physiology during evolution (e.g., a reproductive advantage of male clustering under physiologically challenging conditions).

The mammalian DSK homolog CCK shows sexual dimorphism in brain expression and mating behavior response (51-53). Moreover, CCK activation is implicated in aggression and exploratory behaviors (54, 55). It would thus be interesting to determine whether DSK/CCK signaling indeed represents an ancestral mechanism for social memory, sexually dimorphic social behaviors, and their plasticity.

Materials and Methods

Fly stocks

Flies were raised on standard cornmeal-yeast-agar food at 25°C and 40-50% humidity under 12-h light: 12-h dark cycles. Behavioral experiments were primarily conducted between zeitgeber time (ZT) 4 and 8 (lights-on at ZT0; lights-off at ZT12). DGRP lines, Canton-S (BL64349), *rut*¹ (BL9404), *rut*²⁰⁸⁰ (BL9405), *Dsk*^{attP} (BL84497), *Dsk*^{2A-Gal4} (BL84630), *UAS-Dsk*^{RNAi} (BL25869), *CCKLR-17D1*^{attP} (BL84462), *CCKLR-17D1*^{2A-Gal4} (BL84605), *CCKLR-17D3*^{attP} (BL84463), *Orco*¹ (BL23129), *UAS-myrGFP*.QUAS-mtdTomato-3xHA; trans-Tango (BL77124), 20XUAS-IVS-jGCaMP7f (BL80906), and *UAS-DenMark*, *UAS-syt.eGFP* (BL33065) were obtained from Bloomington Drosophila Stock Center. *CCKLR-17D1*^{Δ1} (119026), *CCKLR-17D1*^{Δ2} (119027), *CCKLR-17D3*^{Δ1} (119029), *CCKLR-17D3*^{Δ2} (119030), *iav*¹ (101174), *norpA*⁷ (108362) and *Poxn*⁶⁸ (119155) were obtained from Kyoto Drosophila Stock Center. *UAS-shi*^{ts}, *UAS-NaChBac*, and *UAS-TNT* have been described previously (47, 56).

SNB analysis

A petri dish [5.5 cm (d) x 1.5 cm (h)] was filled with 2% agar media [1.3 cm (h)] to prepare a circular arena for SNB analysis. This setup minimizes side-wall walking or z-stacking of individual flies that interferes with tracing group behaviors over time (57). Three-to-five-day-old flies from standard cultures (*n* = 16) were briefly cold-anesthetized (< 15 s) and then transferred to the circular arena. Each arena was video-recorded for 10 min using a cellular phone (Samsung Galaxy Note 8 or Samsung Galaxy Note 20). Time-series coordinates of each fly's position in the arena were extracted from raw video data using an in-house Python code (<https://github.com/jiunbae/tracking-fly>). Social distance (SD) was calculated from the position coordinates of individual flies at a given time and averaged over time. The average walking speed of individual flies and the interquartile ranges of the positional centroid in a given group of flies were also calculated over time (https://github.com/KJKwon/2023_FlyBehavior). The centroid velocity was determined from the fourth quarter of video-recording data, given more evident clustering phenotypes at the later period. Single-fly recordings in the circular arena were analyzed using a MATLAB-based fly_tracker code (https://github.com/jstaf/fly_tracker).

Fly manipulations

Drosophila eggs were collected on a plate filled with grape juice media (<https://cshprotocols.cshlp.org/content/2007/9/pdb.rec11113>). Each egg was gently transferred to an isolation chamber containing 300 ul of cornmeal-yeast-agar food for social isolation. The chamber was sealed using parafilm with a tiny hole for air circulation and kept at 25°C before relevant experiments. To generate grouped-to-

isolated (GTI) flies, 3-day-old flies from standard culture vials were individually transferred to each isolation chamber and further incubated for a week. To generate isolated-to-grouped (ITG) flies, 3-day-old flies eclosed from isolated eggs were collected into a standard food vial for group-culturing (~20 isolated flies per vial) and further incubated for a week. To assess SNB in isolated or GTI flies, each fly was reared in the isolation chamber before collectively transferring into the SNB arena. Flies were briefly cold-anesthetized during GTI/ITG transitions or before transferring to the SNB arena. For physical injury, the mesothoracic segment of 3-day-old flies was pierced (< 1-mm depth) using a sterilized needle.

Larval behavior and developmental analyses

For clustering assay, 3rd-instar larvae were obtained from grouped-egg cultures (50 eggs per culture). A group of the 3rd-instar larvae ($n = 20$) were then loaded onto a cylinder vial [2.3 cm (d) x 9.5 cm (h)] containing standard cornmeal-yeast-agar food. The food vial was divided into 4 sectors. The maximum number of clustering larvae per sector was scored from each vial, and the percentage of clusters with given larvae numbers was calculated from 30 vials. For digging assay, a 3D-arena [2 cm (w) x 0.5 cm (d) x 4 cm (h)] was filled up to 2 cm with standard cornmeal-yeast-agar food. Either a group of 3rd-instar larvae ($n = 20$) from standard culture vials or an isolated 3rd-instar larva from single-egg cultures (1 egg per culture) was transferred to the digging-assay arena and then allowed to explore it for 12 h before measuring digging depth from the surface (15). For food intake assay, a wider 3D-arena [8 cm (w) x 0.5 cm (d) x 4 cm (h)] was filled up to 2 cm with standard cornmeal-yeast-agar media containing 1% brilliant blue FCF (JUNSEI, 64350-0410). A group of 3rd-instar larvae ($n = 20$) from standard culture vials or an isolated 3rd-instar larva from single-egg cultures was transferred to the food intake arena and then allowed to explore it for 12 h. Each larva was gently homogenized in 50 μ l of distilled water, and the absorbance of individual larval extracts was measured at 627 nm using a microplate reader (Tecan, Infinite M200). Developmental time was measured by the first eclosion day in a grouped-egg culture (50 eggs per culture) vs. a set of 81 single-egg cultures per experiment. The percentage of eclosed flies was scored from a grouped-egg culture (100 eggs per culture) vs. a set of 81 single-egg cultures per experiment, and the ratio of males to total flies was then calculated accordingly.

Maze assay

Yeast paste was placed at the corner of a 14 cm x 14 cm transparent maze, and the maze was put on a white-light box to avoid any phototactic effects. A group of 4 flies was starved for 6 h and then transferred to the maze by an aspirator. A training session was completed when 3 or more pioneer flies reached the food, and the trained flies were transferred to an empty vial containing water only. The pioneer training was repeated

three times. For the maze test, a group of 16 flies (16 naive or 12 naive + 4 pioneer flies) was briefly cold-anesthetized (< 15 s) and then placed at the opposite corner of the maze to the yeast paste. The 75% arrival time was recorded when 12 or more flies reached the food.

Aggression assay

Quantitative assessment of aggression behaviors was performed as described previously with minor modifications (58). Three-to-five-day-old male flies were separated from females and starved for 6 h. A pair of male flies with the same genotype were then transferred by gentle aspiration into a cylinder arena [1.4 cm (d) x 0.5 cm (h)], where a thin droplet of yeast paste with a decapitated female carcass was placed in the center. The arena was video-recorded for 10 min, and the number of lunges was counted manually.

Courtship chaining behavior assay

Male-male courtship was quantified by the courtship chaining index as described previously with minor modifications (59). A group of three-to-five-day-old male flies ($n = 16$) from standard cultures were briefly cold-anesthetized (< 15 s), transferred to the circular arena for SNB analysis, and then video-recorded for 10 min. Courtship chain was scored when three or more male flies were engaged in chaining with courtship behavior (59). The chaining index was calculated by the percentage of courtship chaining duration over the 10-min recording.

Transcriptome analysis

Three-to-five-day-old flies were harvested at ZT4-6. Total RNAs were extracted from 35 fly heads and purified using the PureLink RNA mini kit according to the manufacturer's instructions (Invitrogen). RNA quality was assessed by Bioanalyzer using the Agilent RNA 6000 pico kit (Agilent Technologies). RNA-seq libraries were constructed using the NEBNext Ultra Directional RNA Library Prep Kit for Illumina (New England Biolabs), together with NEBNext Poly(A) mRNA Magnetic Isolation Module (New England Biolabs) and subsequently sequenced by Illumina NovaSeq 6000 or Illumina NextSeq 500/550 (LabGenomics, Republic of Korea). RNA-seq reads were processed using trimmomatic (60) (version 0.39) with the default option to remove bases with low-quality scores or from sequencing adapters. The trimmed reads were then mapped to the *Drosophila melanogaster* reference genome R6.46 using STAR (61) (version 2.7.10b). Differentially expressed genes were determined using DEseq2 (62) (version 1.40.0; >2 fold change with adjusted $P < 0.05$). Transcripts undetectable in more than half of the RNA-seq libraries were excluded from the analysis. Overrepresented gene ontology terms were identified by Fisher's exact test (false discovery rate < 0.05) with PANTHER (63) (version 17.0).

Quantitative brain imaging

Whole-mount brain imaging was performed as described previously (64). The primary antibodies used in immunostaining included rabbit anti-DSK (Boster Bio, DZ41371; diluted at 0.5 ug/ml) and mouse anti-BRP antibodies (Developmental Studies Hybridoma Bank, nc82; diluted at 1:1,000). The GCaMP signals from live brains were recorded at room temperature using an FV1000 (Olympus) or A1 confocal microscope (Nikon). Fluorescence intensities from regions of interest in confocal images were quantified by background normalization $[(S-B)/B]$ using ImageJ software.

Statistical analysis

Statistical analyses were performed using GraphPad Prism or R (version 4.2.3). Shapiro-Wilk test was followed by F-test (two samples) or Brown-Forsythe test (multiple samples) to check normality ($P < 0.05$) and equality of variances ($P < 0.05$), respectively. For two-sample comparisons, parametric datasets with equal variance were analyzed by unpaired t-test. For multiple-sample comparisons, 1) parametric datasets with equal variance were analyzed by ordinary ANOVA with Tukey's multiple comparisons test; 2) parametric datasets with unequal variance were analyzed by Welch's ANOVA with Dunnett's T3 multiple comparisons test (1-way) or by aligned ranks transformation ANOVA with Wilcoxon rank sum test (2-way); and 3) nonparametric datasets with equal variance were analyzed by Kruskal-Wallis test with Dunn's multiple comparisons test (1-way) or by aligned ranks transformation ANOVA with Wilcoxon rank sum test (2-way). For comparisons between repeatedly measured samples, datasets were analyzed by paired t-test (two samples) or 2-way repeated measures ANOVA with Sidak's multiple comparisons test (multiple samples). The significance of the correlation among SD, walking speed, centroid velocity, food intake, starvation-induced activity, and aggression in DGRP strains was determined by Spearman correlation analysis. Sample sizes and P values obtained from individual statistical analyses were all summarized in each source data and indicated in the figure legends accordingly.

Data, materials, and software availability

The datasets generated and analyzed during the current study are included in each source data or available in the European Nucleotide Archive repository (accession number PRJEB61423). The python scripts that support the findings of this study are available from the author's GitHub webpage under the links <https://github.com/jiunbae/tracking-fly> and https://github.com/KJKwon/2023_FlyBehavior.

Acknowledgments

We thank Bloomington Drosophila Stock Center, Developmental Studies Hybridoma Bank, Korea Drosophila Resource Center, and Kyoto Drosophila Stock Center for reagents; Kenneth Wilson and Pankaj Kapahi for raw data from their phenotypic DGRP screens. This work was supported by grants from the Suh Kyungbae Foundation (SUHF-17020101[C.L.]); from the National Research Foundation funded by the Ministry of Science and Information & Communication Technology (MSIT), Republic of Korea (NRF-2021M3A9G8022960 [C.L.]; NRF-2018R1A5A1024261 [C.L.]; NRF-2023R1A2C100627511 [T.K.]); from Basic Science Research Program through the National Research Foundation funded by Ministry of Education (NRF-2018R1A6A1A03025810 [T.K.]).

Competing Interest Statement

The authors declare no competing interests.

References

1. T. Clutton-Brock, Social evolution in mammals. *Science* **373**, eabc9699 (2021).
2. J. A. Jezovitz, N. Alwash, J. D. Levine, Using Flies to Understand Social Networks. *Front Neural Circuits* **15**, 755093 (2021).
3. M. B. Sokolowski, Social interactions in "simple" model systems. *Neuron* **65**, 780-794 (2010).
4. D. T. Blumstein *et al.*, Toward an integrative understanding of social behavior: new models and new opportunities. *Front Behav Neurosci* **4**, 34 (2010).
5. J. D. Levine, P. Funes, H. B. Dowse, J. C. Hall, Resetting the circadian clock by social experience in *Drosophila melanogaster*. *Science* **298**, 2010-2012 (2002).
6. I. Ganguly-Fitzgerald, J. Donlea, P. J. Shaw, Waking experience affects sleep need in *Drosophila*. *Science* **313**, 1775-1781 (2006).
7. R. G. Arzate-Mejia, Z. Lottenbach, V. Schindler, A. Jawaid, I. M. Mansuy, Long-Term Impact of Social Isolation and Molecular Underpinnings. *Front Genet* **11**, 589621 (2020).
8. W. Li *et al.*, Chronic social isolation signals starvation and reduces sleep in *Drosophila*. *Nature* **597**, 239-244 (2021).
9. M. Chen, M. B. Sokolowski, How Social Experience and Environment Impacts Behavioural Plasticity in *Drosophila*. *Fly (Austin)* **16**, 68-84 (2022).
10. A. Vora, A. D. Nguyen, C. Spicer, W. Li, The impact of social isolation on health and behavior in *Drosophila melanogaster* and beyond. *Brain Science Advances* **8**, 183-196 (2022).
11. Y. Xiong, H. Hong, C. Liu, Y. Q. Zhang, Social isolation and the brain: effects and mechanisms. *Mol Psychiatry* **28**, 191-201 (2023).
12. J. Schneider, M. H. Dickinson, J. D. Levine, Social structures depend on innate determinants and chemosensory processing in *Drosophila*. *Proc Natl Acad Sci U S A* **109** Suppl 2, 17174-17179 (2012).
13. A. F. Simon *et al.*, A simple assay to study social behavior in *Drosophila*: measurement of social space within a group. *Genes Brain Behav* **11**, 243-252 (2012).
14. P. Ramdya *et al.*, Mechanosensory interactions drive collective behaviour in *Drosophila*. *Nature* **519**, 233-236 (2015).
15. M. Dombrovski *et al.*, Cooperative Behavior Emerges among *Drosophila* Larvae. *Curr Biol* **27**, 2821-2826 e2822 (2017).
16. Y. Sun *et al.*, Social attraction in *Drosophila* is regulated by the mushroom body and serotonergic system. *Nat Commun* **11**, 5350 (2020).
17. E. D. Burg, S. T. Langan, H. A. Nash, *Drosophila* social clustering is disrupted by anesthetics and in narrow abdomen ion channel mutants. *Genes Brain Behav* **12**, 338-347 (2013).
18. A. Bentzur *et al.*, Early Life Experience Shapes Male Behavior and Social Networks in *Drosophila*. *Curr Biol* **31**, 670 (2021).
19. L. Jiang *et al.*, Emergence of social cluster by collective pairwise encounters in *Drosophila*. *Elife* **9** (2020).
20. T. F. Mackay *et al.*, The *Drosophila melanogaster* Genetic Reference Panel. *Nature* **482**, 173-178 (2012).
21. T. F. C. Mackay, W. Huang, Charting the genotype-phenotype map: lessons from the *Drosophila melanogaster* Genetic Reference Panel. *Wiley Interdiscip Rev Dev Biol* **7** (2018).
22. V. Gardeux *et al.* (2023) DGRPpool: A web tool leveraging harmonized *Drosophila* Genetic Reference Panel phenotyping data for the study of complex traits. (eLife Sciences Publications, Ltd).

- 616 23. B. Horvath, A. T. Kalinka, Effects of larval crowding on quantitative variation for
617 development time and viability in *Drosophila melanogaster*. *Ecol Evol* **6**, 8460-8473
618 (2016).
- 619 24. P. Klepsatel, E. Prochazka, M. Galikova, Crowding of *Drosophila* larvae affects lifespan
620 and other life-history traits via reduced availability of dietary yeast. *Exp Gerontol* **110**,
621 298-308 (2018).
- 622 25. L.-A. Giraldeau, T. Caraco, *Social foraging theory*, Monographs in behavior and ecology
623 (Princeton University Press, Princeton, N.J., 2000), pp. xiii, 362 p.
- 624 26. L. R. Levin *et al.*, The *Drosophila* learning and memory gene rutabaga encodes a
625 Ca²⁺/Calmodulin-responsive adenylyl cyclase. *Cell* **68**, 479-489 (1992).
- 626 27. L. Wang, H. Dankert, P. Perona, D. J. Anderson, A common genetic target for
627 environmental and heritable influences on aggressiveness in *Drosophila*. *Proc Natl Acad Sci U S A* **105**, 5657-5663 (2008).
- 629 28. P. Agrawal, D. Kao, P. Chung, L. L. Looger, The neuropeptide Drosulfakinin regulates
630 social isolation-induced aggression in *Drosophila*. *J Exp Biol* **223** (2020).
- 631 29. J. A. Jezovit, R. Rooke, J. Schneider, J. D. Levine, Behavioral and environmental
632 contributions to drosophilid social networks. *Proc Natl Acad Sci U S A* **117**, 11573-11583
633 (2020).
- 634 30. G. Liu *et al.*, A simple computer vision pipeline reveals the effects of isolation on social
635 interaction dynamics in *Drosophila*. *PLoS Comput Biol* **14**, e1006410 (2018).
- 636 31. M. E. Garlapow, W. Huang, M. T. Yarboro, K. R. Peterson, T. F. Mackay, Quantitative
637 Genetics of Food Intake in *Drosophila melanogaster*. *PLoS One* **10**, e0138129 (2015).
- 638 32. J. Shorter *et al.*, Genetic architecture of natural variation in *Drosophila melanogaster*
639 aggressive behavior. *Proc Natl Acad Sci U S A* **112**, E3555-3563 (2015).
- 640 33. W. Chi *et al.*, RNA-binding protein syncrip regulates starvation-induced hyperactivity in
641 adult *Drosophila*. *PLoS Genet* **17**, e1009396 (2021).
- 642 34. S. Wu *et al.*, Drosulfakinin signaling in fruitless circuitry antagonizes P1 neurons to
643 regulate sexual arousal in *Drosophila*. *Nat Commun* **10**, 4770 (2019).
- 644 35. F. Wu *et al.*, A neuropeptide regulates fighting behavior in *Drosophila melanogaster*.
645 *Elife* **9** (2020).
- 646 36. D. Guo *et al.*, Cholecystokinin-like peptide mediates satiety by inhibiting sugar attraction.
647 *PLoS Genet* **17**, e1009724 (2021).
- 648 37. T. Wang *et al.*, Drosulfakinin signaling modulates female sexual receptivity in *Drosophila*.
649 *Elife* **11** (2022).
- 650 38. R. Nichols, S. A. Schneuwly, J. E. Dixon, Identification and characterization of a
651 *Drosophila* homologue to the vertebrate neuropeptide cholecystokinin. *J Biol Chem* **263**,
652 12167-12170 (1988).
- 653 39. D. Staljanssens *et al.*, The CCK(-like) receptor in the animal kingdom: functions,
654 evolution and structures. *Peptides* **32**, 607-619 (2011).
- 655 40. D. R. Nassel, S. F. Wu, Cholecystokinin/sulfakinin peptide signaling: conserved roles at
656 the intersection between feeding, mating and aggression. *Cell Mol Life Sci* **79**, 188
657 (2022).
- 658 41. M. Talay *et al.*, Transsynaptic Mapping of Second-Order Taste Neurons in Flies by
659 trans-Tango. *Neuron* **96**, 783-795 e784 (2017).
- 660 42. A. Sorkac *et al.*, retro-Tango enables versatile retrograde circuit tracing in *Drosophila*.
661 *Elife* **12**, e85041 (2023).
- 662 43. F. Wu *et al.*, A neuropeptide regulates fighting behavior in *Drosophila melanogaster*.
663 *Elife* **9**, e54229 (2020).
- 664 44. I. Oikawa *et al.*, A descending inhibitory mechanism of nociception mediated by an
665 evolutionarily conserved neuropeptide system in *Drosophila*. *Elife* **12** (2023).

45. J. A. Soderberg, M. A. Carlsson, D. R. Nassel, Insulin-Producing Cells in the Drosophila Brain also Express Satiety-Inducing Cholecystokinin-Like Peptide, Drosulfakinin. *Front Endocrinol (Lausanne)* **3**, 109 (2012).
46. M. J. Williams *et al.*, Obesity-linked homologues TfAP-2 and Twz establish meal frequency in Drosophila melanogaster. *PLoS Genet* **10**, e1004499 (2014).
47. T. Kitamoto, Conditional modification of behavior in Drosophila by targeted expression of a temperature-sensitive shibire allele in defined neurons. *J Neurobiol* **47**, 81-92 (2001).
48. D. J. Anderson, Circuit modules linking internal states and social behaviour in flies and mice. *Nat Rev Neurosci* **17**, 692-704 (2016).
49. S. P. Nilsen, Y. B. Chan, R. Huber, E. A. Kravitz, Gender-selective patterns of aggressive behavior in Drosophila melanogaster. *Proc Natl Acad Sci U S A* **101**, 12342-12347 (2004).
50. J. C. Simon, U. Heberlein, Social hierarchy is established and maintained with distinct acts of aggression in male Drosophilamelanogaster. *J Exp Biol* **223** (2020).
51. G. J. Bloch, A. M. Babcock, R. A. Gorski, P. E. Micevych, Cholecystokinin stimulates and inhibits lordosis behavior in female rats. *Physiol Behav* **39**, 217-224 (1987).
52. G. J. Bloch, A. M. Babcock, R. A. Gorski, P. E. Micevych, Effects of cholecystokinin on male copulatory behavior and lordosis behavior in male rats. *Physiol Behav* **43**, 351-357 (1988).
53. P. Micevych, T. Akesson, R. Elde, Distribution of cholecystokinin-immunoreactive cell bodies in the male and female rat: II. Bed nucleus of the stria terminalis and amygdala. *J Comp Neurol* **269**, 381-391 (1988).
54. S. Raud *et al.*, Targeted invalidation of CCK2 receptor gene induces anxiolytic-like action in light-dark exploration, but not in fear conditioning test. *Psychopharmacology (Berl)* **181**, 347-357 (2005).
55. Q. Li, X. Deng, P. Singh, Significant increase in the aggressive behavior of transgenic mice overexpressing peripheral progastrin peptides: associated changes in CCK2 and serotonin receptors in the CNS. *Neuropsychopharmacology* **32**, 1813-1821 (2007).
56. M. N. Nitabach *et al.*, Electrical hyperexcitation of lateral ventral pacemaker neurons desynchronizes downstream circadian oscillators in the fly circadian circuit and induces multiple behavioral periods. *J Neurosci* **26**, 479-489 (2006).
57. J. C. Simon, M. H. Dickinson, A new chamber for studying the behavior of Drosophila. *PLoS One* **5**, e8793 (2010).
58. S. Chen, A. Y. Lee, N. M. Bowens, R. Huber, E. A. Kravitz, Fighting fruit flies: a model system for the study of aggression. *Proc Natl Acad Sci U S A* **99**, 5664-5668 (2002).
59. T. Kitamoto, Conditional disruption of synaptic transmission induces male-male courtship behavior in Drosophila. *Proc Natl Acad Sci U S A* **99**, 13232-13237 (2002).
60. A. M. Bolger, M. Lohse, B. Usadel, Trimmomatic: a flexible trimmer for Illumina sequence data. *Bioinformatics* **30**, 2114-2120 (2014).
61. A. Dobin *et al.*, STAR: ultrafast universal RNA-seq aligner. *Bioinformatics* **29**, 15-21 (2013).
62. M. I. Love, W. Huber, S. Anders, Moderated estimation of fold change and dispersion for RNA-seq data with DESeq2. *Genome Biol* **15**, 550 (2014).
63. P. D. Thomas *et al.*, PANTHER: Making genome-scale phylogenetics accessible to all. *Protein Sci* **31**, 8-22 (2022).
64. J. Jeong, J. Lee, J. H. Kim, C. Lim, Metabolic flux from the Krebs cycle to glutamate transmission tunes a neural brake on seizure onset. *PLoS Genet* **17**, e1009871 (2021).

Figure Legends

Figure 1. Social network behavior is a quantitative trait in a natural *Drosophila* population. (A) The 10-min video recording of social network behavior (SNB) in a group of 16 male flies. Representative snapshot images at each quarter time point (Q1, Q2, Q3, and Q4) were obtained from *Drosophila* strains with high (top, short SD) or low clustering properties (bottom, long SD). (B) The definition of social distance (SD). SD was measured in each fly over the 10-min recording and averaged from a given group. Representative SD dynamics from short- (top) or long-SD strains (bottom) were shown. Dotted lines, group-averaged SD over the 10-min recordings. (C) Quantitative assessment of SNB by ranking SD, walking speed, and centroid velocity among 175 DGRP lines. Data represent means \pm SEM ($n = 5$). (D) Significant correlation among SD, walking speed, and centroid velocity. $***P < 0.001$, as determined by Spearman correlation analysis. Red, representative short-SD lines; blue, representative long-SD lines.

The online version of this article provides the following source data for Figure 1:
Figure 1—source data 1. Correlation of SD, walking speed, and centroid velocity across 175 DGRP lines.

Figure 2. Short- and long-SD lines exhibit distinct SNB. (A, B) SNB dynamics in short-SD (A) and long-SD lines (B). SD dynamics in a representative group of 16 male flies over the 10-min recordings (left, $n = 16$), quarter-averaged SD (middle, $n = 8$), and quarter-averaged walking speed (right, $n = 8$) were shown for each DGRP line. Error bars indicate SEM. n.s., not significant; $*P < 0.05$, $**P < 0.01$, $***P < 0.001$ as determined by paired t-test (DGRP73, DGRP563, DGRP370, DGRP707, and DGRP317 for quarter-averaged SD; DGRP563, DGRP360, and DGRP317 for quarter-averaged walking speed) or Wilcoxon matched-pairs signed rank test (DGRP360 for quarter-averaged SD; DGRP73, DGRP370, and DGRP707 for quarter-averaged walking speed). (C) The 10-min locomotion trajectories of representative individual flies from short- (red) or long-SD lines (blue). (D) Cumulative travel distances of individual flies over the 10-min recording. Colored lines represent means ($n = 128$).

The online version of this article provides the following source data and figure supplements for Figure 2:
Figure 2—source data 1. Quantitative locomotor metrics in short- and long-SD DGRP lines.
Figure 2—figure supplement 1. Social network behaviors in the three representative DGRP lines displaying short or long SD.

Figure 2—figure supplement 2. Neither short- nor long-SD lines reduce their walking speeds over time when individual flies from group cultures are isolated.

Figure 2—figure supplement 3. The clustering property of each DGRP line persists in a large arena.

Figure 2—figure supplement 4. Neither short- or long-SD lines display male-male courtship behavior.

Figure 2—figure supplement 1. Social network behaviors in the three representative DGRP lines displaying short or long SD. (A) Centroid trajectories of short- (red; DGRP73, 563, 370) or long-SD lines (blue; DGRP360, 707, 317) over the 10-min video recording. (B) The short-SD lines exhibit slow walking speeds and low centroid velocities compared to the long-SD lines. Social isolation significantly impaired SNB only in the short-SD lines. Data represent means \pm SEM ($n = 8$). n.s., not significant; $*P < 0.05$, $**P < 0.01$, $***P < 0.001$, as determined by unpaired t-test. (C) Long-SD individuals show longer travel distances than short-SD ones during the 10-min video recording. Data represent means \pm SEM ($n = 8$ for averaged data; $n = 128$ for individual data). $***P < 0.001$ as determined by ordinary 1-way ANOVA with Tukey's multiple comparisons test (averaged data) or aligned ranks transformation ANOVA with Wilcoxon rank-sum test (individual data).

Figure 2—figure supplement 2. Neither short- nor long-SD lines reduce their walking speeds over time when individual flies from group cultures are isolated. A single male fly from each DGRP line was placed in the arena for SNB analysis and video-recorded for 10 min to quantify its locomotor activity. Data represent means \pm SEM ($n = 20$). n.s., not significant; $*P < 0.05$, $**P < 0.01$, as determined by Wilcoxon matched-pairs signed rank test (DGRP73, DGRP563, DGRP370, and DGRP360) or paired t test (DGRP707 and DGRP317).

Figure 2—figure supplement 3. The clustering property of each DGRP line persists in a large arena. A group of 16 male flies was placed in a large arena (8.5 cm in diameter), and their locomotor behaviors were video-recorded for 10 min. Representative snapshot images were obtained at each quarter of the 10-min recording. The heatmap illustrates the relative distribution of individual flies in the arena.

Figure 2—figure supplement 4. Neither short- or long-SD lines display male-male courtship behavior. (A) A representative snapshot image of courtship chaining behavior (dotted circle) in a group of *rut¹* mutant flies. (B) The chaining index was calculated from the 10-min video-recording of 16 male flies in the arena. Data represent means \pm SEM ($n = 8$). DGRP lines did not display any detectable courtship chaining behavior.

Figure 3. Early-life social experience confers beneficial effects on *Drosophila* development. (A) Larval clustering in short- (red) or long-SD lines (blue). % clusters were calculated from 30 vials. Arrows indicate individual larvae. Scale bar = 0.5 mm. (B) Schematic for grouped (grp) vs. developmentally isolated (iso) culture conditions. (C, D) Grouped culture compensated for low food accessibility in the short-SD larvae. Aligned ranks transformation ANOVA detected significant effects of SD trait and social isolation on both digging depth (C, $P < 0.0001$) and food intake (D, $P < 0.0001$), and their significant interaction effects were detected only on digging depth (C, $P = 0.0338$). Data represent means \pm SEM ($n = 36$; 12 per line \times 3 lines). *** $P < 0.001$, as determined by Wilcoxon rank sum test. (E-G) Grouped culture rescued developmental delay and low male-progeny ratio in the short-SD larvae. Aligned ranks transformation ANOVA or ordinary 2-way ANOVA detected significant effects of SD trait and social isolation on developmental time (E, $P < 0.0001$), eclosion success (F, $P = 0.0116$ for SD trait; $P < 0.0001$ for social isolation), and male progeny ratio (G, $P < 0.0001$). Significant interaction effects between SD trait and social isolation were also detected on developmental time (E, $P < 0.0001$) and male progeny ratio (G, $P < 0.0001$). Data represent means \pm SEM ($n = 24$; 8 per line \times 3 lines). n.s., not significant; * $P < 0.05$, *** $P < 0.001$, as determined by Wilcoxon rank sum test (developmental time and male progeny ratio) or Tukey's multiple comparisons test (eclosion success).

The online version of this article provides the following source data for Figure 3:
Figure 3—source data 1. Quantitative analysis of larval SNB and developmental metrics.

Figure 4. Early-life social experience confers beneficial effects on social foraging in adult *Drosophila*. (A) Experimental scheme for assessing social interactions in a maze assay. Representative images were shown for a group of *Drosophila* strains with high (short latency) or low social foraging (long latency). (B) Pioneer groups of flies from either grouped (grp) or isolated cultures (iso) were effectively trained in the maze assay, but social isolation of both short- (red, DGRP73) and long-SD flies (blue, DGRP360) blunted the pioneer effects on food-seeking behaviors in a group of naive flies. Two-way repeated measures ANOVA detected significant effects of training ($P < 0.0001$ for DGRP73 and DGRP360) but not social isolation on latency during the training session of pioneer groups. Ordinary 2-way ANOVA also detected significant interaction effects of pioneer and social isolation on latency during the maze test ($P = 0.0131$ for DGRP73; $P = 0.0310$ for DGRP360). Data represent means \pm SEM ($n = 6$ –16). n.s., not significant; * $P < 0.05$, ** $P < 0.01$, *** $P < 0.001$, as determined by Sidak's multiple comparisons test (training session) or Tukey's multiple comparisons test (maze test). (C) Experimental scheme for assessing injury-induced SNB plasticity. GTI, grouped-to-isolated culture transition; ITG, isolated-to-grouped culture transition. (D) Physical injury induced

clustering behaviors in group-cultured but not developmentally isolated flies. Data represent means \pm SEM ($n = 8$). n.s., not significant; $*P < 0.05$, $**P < 0.01$, $***P < 0.001$, as determined by 1-way ANOVA with Tukey's multiple comparisons test.

The online version of this article provides the following source data and figure supplements for Figure 4:

Figure 4—source data 1. Quantitative analysis of adult SNB and social plasticity.

Figure 4—figure supplement 1. Social isolation blunts pioneer effects on food-seeking behaviors in a group of naive flies.

Figure 4—figure supplement 2. *rutabaga*-dependent working memory is dispensable for social memory.

Figure 4—figure supplement 3. Early-life social experience is necessary for social behavior plasticity in male flies.

Figure 4—figure supplement 4. Mechanical injury reduces walking speed and centroid velocity only in group-cultured long-SD flies.

Figure 4—figure supplement 5. Loss of *norpA* function blocks injury-induced clustering in group-cultured male flies.

Figure 4—figure supplement 1. Social isolation blunts pioneer effects on food-seeking behaviors in a group of naive flies. Pioneer groups of short- (DGRP563 and DGRP370) and long-SD lines (DGRP707 and DGRP317) were effectively trained in the maze assay but they failed to improve the efficiency of food-seeking behaviors with groups of socially isolated flies. Data represent means \pm SEM ($n = 6-12$). n.s., not significant; $*P < 0.05$, $**P < 0.01$, $***P < 0.001$, as determined by 2-way repeated measures ANOVA with Sidak's multiple comparisons test (pioneer training) or 2-way ANOVA with Tukey's multiple comparisons test (group test). Grp, grouped; iso, isolated.

Figure 4—figure supplement 2. *rutabaga*-dependent working memory is dispensable for social memory. (A) Plasticity mutants of *rutabaga* (*rut*¹ and *rut*²⁰⁸⁰) fail to improve food-seeking behaviors in the maze after repetitive trainings. Canton-S (CS) served as a wild-type control. Data represent means \pm SEM ($n = 9$ for *rut*¹; $n = 8$ for *rut*²⁰⁸⁰). n.s., not significant; $**P < 0.01$, $***P < 0.001$, as determined by paired t-test. (B) *rut* mutants display injury-induced clustering comparable to control flies. SD was measured in group-cultured male flies under distinct experimental conditions (ctrl, control; inj, injured). Two-way ANOVA detected no significant interaction effects of genotype and inj on SD. Data represent means \pm SEM ($n = 8$ for *rut*¹; $n = 10$ for *rut*²⁰⁸⁰). $*P < 0.05$, $**P < 0.01$, as determined by Tukey's multiple comparisons test.

Figure 4—figure supplement 3. Early-life social experience is necessary for social behavior plasticity in male flies. (A) Physical injury induced clustering behaviors in

group-cultured but not developmentally isolated flies. SD was measured in a group of male flies under distinct experimental conditions (ctrl, control; inj, injured; rec, recovered; grp, grouped; iso, isolated; GTI, grouped-to-isolated culture transition; ITG, isolated-to-grouped culture transition). Data represent means \pm SEM ($n = 8$). n.s., not significant; $*P < 0.05$, $**P < 0.01$, $***P < 0.001$, as determined by 1-way ANOVA with Tukey's multiple comparisons test. (B) Female flies did not display injury-induced clustering. SD was measured in group-cultured female flies from individual DGRP lines. Data represent means \pm SEM ($n = 8$). n.s., not significant as determined by 1-way ANOVA with Tukey's multiple comparisons test.

Figure 4—figure supplement 4. Mechanical injury reduces walking speed and centroid velocity only in group-cultured long-SD flies. Locomotor activities were quantified in a group of long- and short-SD male flies under distinct experimental conditions (ctrl, control; inj, injured; rec, recovered; grp, grouped; iso, isolated). Two-way ANOVA detected significant interaction effects of inj and iso on walking speed and centroid velocity only in long-SD lines ($***P < 0.001$ for DGRP360 and DGRP707; $*P < 0.05$ for DGRP317, except centroid velocity). Data represent means \pm SEM ($n = 8$). n.s., not significant; $*P < 0.05$, $**P < 0.01$, $***P < 0.001$, as determined by Tukey's multiple comparisons test.

Figure 4—figure supplement 5. Loss of *norpA* function blocks injury-induced clustering in group-cultured male flies. SD was measured in a group of male mutants for each sensory-pathway gene as described in Figure 1. Data represent means \pm SEM ($n = 8$). n.s., not significant; $*P < 0.05$, $**P < 0.01$, $***P < 0.001$, as determined by 2-way ANOVA with Tukey's multiple comparisons test. Ctrl, control; inj, injured.

Figure 5. Social experience shapes gene expression profiles in *Drosophila* heads. (A) Heatmaps for differentially expressed genes (DEGs, > 2 -fold difference with adjusted $P < 0.05$) in short- vs. long-SD lines (left); in grouped (grp) vs. isolated (iso) condition (right). Fly heads were harvested from individual DGRP lines in grouped or isolated cultures and their gene expression profiles were analyzed by RNA sequencing. Averaged counts per million were converted to z-score for visualization. (B) Volcano plots for DEGs in short- vs. long-SD lines (top); in grp vs. iso flies (bottom). Social interactions evidently upregulated the neuropeptide *Drosulfakinin* (*Dsk*) expression. (C) Overlapping DEGs in grp vs. iso conditions across DGRP lines. *Dsk* was identified as a commonly upregulated gene by social interactions in short- (top, red) and long-SD lines (middle, blue). (D) Gene ontology analysis reveals upregulation of select metabolic pathways upon social isolation. False discovery rate (FDR) < 0.05 , as determined by Fisher's exact test (grp vs. iso). (E) Significant phenotypic correlation of SNB to food

intake, starvation-induced activity, and mean aggressive encounters among DGRP lines. Raw data for food intake ($n = 52$ DGRP lines), starvation-induced activity ($n = 60$ DGRP lines), and aggression ($n = 57$ DGRP lines) were obtained from previous studies (31-33) and then aligned to SD, centroid velocity, and walking speed in the corresponding DGRP lines that were measured by our SNB analyses. $*P < 0.05$, $**P < 0.01$, $***P < 0.001$, as determined by Spearman correlation analysis. (F) Expression heatmap for genes implicated in feeding, adult locomotor behavior, and aggression. Downregulation of *Dsk* and its two receptors (CCKLR-17D1 and CCKLR-17D3) by social isolation was visualized in relevant gene categories.

The online version of this article provides the following source data and figure supplements for Figure 5:

Figure 5—source data 1. Normalized gene expression in individual DGRP lines under grouped vs. isolated culture conditions.

Figure 5—source data 2. DEG analyses between distinct social groups (short vs. long SD; or grouped vs. isolated).

Figure 5—source data 3. Comparative analyses of social group-specific DEGs from independent studies.

Figure 5—source data 4. DEG analyses among individual DGRP lines.

Figure 5—source data 5. Correlation of SNB to food intake, starvation-induced activity, and aggression among DGRP lines.

Figure 5—figure supplement 1. Cross-study analyses of social context-dependent DEGs highlight *Dsk* as the most prominently up-regulated gene under socially enriched conditions.

Figure 5—figure supplement 2. Long-SD flies display higher aggression than short-SD flies.

Figure 5—figure supplement 1. Cross-study analyses of social context-dependent DEGs highlight *Dsk* as the most prominently up-regulated gene under socially enriched conditions. (A) Venn diagrams depict the numbers of up-regulated genes under grouped (top, grp) and socially isolated conditions (bottom, iso), as identified by the previous and current studies. The numbers of overlapping DEGs between independent gene expression analyses were shown accordingly. (B) Venn diagrams illustrate the overlap of DEGs between short-SD lines and group-culturing conditions (top, short SD vs. grp) and between long-SD lines and socially isolated conditions (bottom, long SD vs. iso).

Figure 5—figure supplement 2. Long-SD flies display higher aggression than short-SD flies. A pair of male flies from each DGRP line were starved for 6 h and then placed into a circular arena with yeast paste and a female carcass in the center. The

number of lunges was counted during the 10-min video recording. Data represent means \pm SEM ($n = 6$). $*P < 0.05$, as determined by 1-way ANOVA with Tukey's multiple comparisons test.

Figure 6. DSK neuron activity encodes social experience. (A and B) Social experience elevates DSK levels in the *Drosophila* brains. Whole-mount brains from each DGRP line in grouped (grp) or socially isolated cultures (iso) were co-immunostained with anti-DSK (green) and anti-BRUCHPILOT antibodies (BRP, a synaptic protein; magenta). The fluorescent DSK signals from confocal images were quantified using ImageJ. Ordinary 2-way ANOVA or aligned ranks transformation ANOVA detected significant effects of social isolation on DSK levels in MP1a/MP1b/MP3 cell bodies and their projections ($P < 0.0001$). The SD trait effects (i.e., short vs. long SD) were more evident on DSK levels in cell bodies ($P < 0.0001$). Data represent means \pm SEM ($n = 13$). n.s., not significant; $**P < 0.01$, $***P < 0.001$, as determined by Tukey's multiple comparisons test (MP1a/MP1b cell bodies and MP1a projections) or Wilcoxon rank sum test (MP3 cell bodies and projections). Scale bar = 40 μ m. (C) Social experience and physical injury elevate DSK neuron activity. Social isolation masked an injury-induced Ca^{2+} increase in the MP1a neurons among other DSK neurons as assessed by the genetically encoded Ca^{2+} sensor GCaMP in live-brain imaging. Two-way ANOVA detected significant effects of social isolation ($P < 0.0001$) and injury (inj, $P < 0.01$) on GCaMP levels in DSK neurons. Data represent means \pm SEM ($n = 10$). n.s., not significant; $*P < 0.05$, $**P < 0.01$, $***P < 0.001$, as determined by Tukey's multiple comparisons test. Scale bar = 5 μ m. (D-F) Social experience strengthens postsynaptic signaling of DSK neurons only in males. Whole-mount brains were dissected from group-cultured (grp) or isolated (iso) flies and immunostained with anti-DSK antibody (white). Postsynaptic partner of DSK neurons was visualized by the heterologous ligand-receptor signaling embedded in the transsynaptic mapping transgene (*Dsk*>trans-Tango, magenta) while DSK neurons were further labeled by the presynaptic marker of the trans-Tango (green). The fluorescent trans-Tango signals and anti-DSK staining intensities from confocal images were quantified using ImageJ. Aligned ranks transformation ANOVA or ordinary 2-way ANOVA detected significant interaction effects of social isolation and gender on trans-Tango signals (E, $P < 0.0001$) and DSK levels in MP1a projection (F, $P < 0.0001$). Data represent means \pm SEM ($n = 13$). n.s., not significant; $***P < 0.001$, as determined by Wilcoxon rank sum test (trans-Tango signals) or Tukey's multiple comparisons test (DSK levels). Scale bar = 40 μ m.

The online version of this article provides the following source data and figure supplements for Figure 6:

Figure 6—source data 1. Quantitative analysis of DSK neuron activities under distinct social contexts.

Figure 6—figure supplement 1. Neither social experience nor physical injury affects transgenic DenMark expression in DSK neurons.

Figure 6—figure supplement 2. Neither social experience nor physical injury affects circadian-clock neuron activity.

Figure 6—figure supplement 1. Neither social experience nor physical injury affects transgenic DenMark expression in DSK neurons. (A) Transgenic *Dsk*-Gal4 flies (*Dsk*>GCaMP7f and *Dsk*>DenMark+SytGFP) and heterozygous controls (*Dsk*-Gal4/+) display social experience-dependent plasticity of SNB.

SD was measured in a group of transgenic male flies under distinct experimental conditions (ctrl, control; inj, injured; grp, grouped; iso, isolated). Data represent means \pm SEM ($n = 8$). n.s., not significant; *** $P < 0.001$, as determined by 2-way ANOVA with Tukey's multiple comparisons test. (B) Dendrites (DenMark, magenta) and axons (SytGFP, green) in DSK neurons were visualized by confocal imaging of a whole-mount transgenic brain (*Dsk*>DenMark +SytGFP). Scale bar = 40 μ m. (C) Social isolation or mechanical injury did not affect the transgenic DenMark expression in DSK neurons. The fluorescence intensities of the DenMark signals in DSK neurons were quantified from confocal images using ImageJ. Data represent means \pm SEM ($n = 6$). n.s., not significant as determined by 2-way ANOVA with Tukey's multiple comparisons test. Dotted lines indicate ROI. Scale bar = 5 μ m.

Figure 6—figure supplement 2. Neither social experience nor physical injury affects circadian-clock neuron activity. (A) Circadian-clock neurons expressing the neuropeptide Pigment-dispersing factor were visualized in whole-mount adult brain by the combination of *Pdf*-Gal4 driver and red fluorescent protein transgenes (*Pdf*>mRFP). Arrows in each hemisphere indicate PDF-expressing large ventral lateral neurons (l-LNV). Scale bar = 40 μ m. (B) The genetically encoded Ca^{2+} sensor GCaMP was expressed by the *Pdf*-Gal4 driver (*Pdf*>GCaMP7f) and the transgenic flies were harvested under distinct experimental conditions (ctrl, control; inj, injured; grp, grouped; iso, isolated). Live-brain Ca^{2+} imaging was then conducted in dissected brains. The GCaMP signals in l-LNV were quantified using ImageJ. Data represent means \pm SEM ($n = 5$). n.s., not significant as determined by 2-way ANOVA with Tukey's multiple comparisons test. Scale bar = 5 μ m.

Figure 7. Genetic manipulations of DSK signaling imitate social experience. (A) *Dsk*^{attP} mutant brain expresses barely detectable DSK peptides. Whole-mount brains from Canton S (CS, a wild-type control) and *Dsk*^{attP} mutant flies were co-immunostained with anti-DSK (green) and anti-BRUCHPILOT antibodies (BRP, a synaptic protein; magenta). Scale bar = 40 μ m. (B and C) Genetic silencing of DSK-CCKLR-17D1 signaling by genomic deletions (*Dsk*^{attP} or *CCKLR-17D1*^{attP}) or DSK depletion

(*Dsk>Dsk^{RNAi}*) blocks injury-induced clustering behaviors. Data represent means \pm SEM ($n = 8$). n.s., not significant; $**P < 0.01$, $***P < 0.001$, as determined by 2-way ANOVA with Tukey's multiple comparisons test. (D and E) Conditional blockade of DSK neuron transmission at larval stage is sufficient to blunt social experience-dependent plasticity of SNB. Transgenic crosses for DSK-specific expression of the temperature sensitive *shibire* allele (*Dsk>shi^{ts}*) were kept at either restrictive (29°C) or permissive temperature (18°C) for synaptic transmission until the end of larval stage. Two-way ANOVA detected significant interaction effects of injury (inj) and temperature on SD in *Dsk>shi^{ts}* flies ($P = 0.0169$) but not in heterozygous controls ($P = 0.7549$ for *Dsk-Gal4/+*; $P = 0.2030$ for *shi^{ts}/+*). Data represent means \pm SEM ($n = 6$). n.s., not significant; $*P < 0.05$, $**P < 0.01$, $***P < 0.001$, as determined by Tukey's multiple comparisons test. (F) CCKLR-17D1 neurons display sexually dimorphic dendrites around MP1 projections. Transgenic male or female brains (*CCKLR-17D1>DenMark+SytGFP*) were immunostained with anti-DSK antibody to visualize DSK neuron projections (white) along with dendrites (DenMark, magenta) and axons (SytGFP, green) of neurons expressing CCKLR-17D1-Gal4 knock-in. Scale bar = 40 μ m. (G) Transgenic excitation of CCKLR-17D1 neurons confers injury-induced plasticity of SNB in socially isolated males but not females. Two-way ANOVA detected significant interaction effects of injury (inj) and social isolation on SD in male heterozygous controls ($P = 0.0040$ for *17D1-Gal4/+*; $P = 0.0007$ for *NaChBac/+*) but not in all the other genotypes. Data represent means \pm SEM ($n = 8$). n.s., not significant; $*P < 0.05$, $**P < 0.01$, as determined by Tukey's multiple comparisons test.

The online version of this article provides the following source data and figure supplements for Figure 7:

Figure 7—source data 1. Quantitative analysis of SNB plasticity in genetic and transgenic *Drosophila* models for DSK-DSK receptor signaling.

Figure 7—figure supplement 1. Transgenic *Dsk* RNAi effectively depletes DSK peptides in the adult brain.

Figure 7—figure supplement 2. Genomic deletions of *CCKLR-17D1* but not *CCKLR-17D3* suppress injury-induced clustering in group-cultured male flies.

Figure 7—figure supplement 3. Transgenic silencing of CCKLR-17D1 neurons suppresses injury-induced clustering in group-cultured male flies.

Figure 7—figure supplement 1. Transgenic *Dsk* RNAi effectively depletes DSK peptides in the adult brain. The *Dsk* RNAi transgene was expressed in DSK neurons by the *Dsk-Gal4* knock-in driver (*Dsk>Dsk^{RNAi}*). Whole-mount transgenic brains were co-immunostained with anti-DSK (green) and anti-BRP (magenta) antibodies. Heterozygous flies for Gal4 (*Dsk-Gal4/+*) or RNAi transgenes (*Dsk^{RNAi}/+*) served as negative controls. Scale bar = 40 μ m

Figure 7—figure supplement 2. Genomic deletions of *CCKLR-17D1* but not *CCKLR-17D3* suppress injury-induced clustering in group-cultured male flies. Deletion mutants of the two *Dsk* receptor genes (*CCKLR-17D1* and *CCKLR-17D3*) and hemizygous control flies (+/Y) were obtained from standard group cultures. SD was measured in a group of male flies as described in Figure 1. Two-way ANOVA detected significant interaction effects of injury (inj) with *CCKLR-17D1* deletions ($P = 0.0404$ for *CCKLR-17D1*^{Δ1}; $P = 0.0254$ for *CCKLR-17D1*^{Δ2}) but not with *CCKLR-17D3* deletions ($P = 0.1051$ for *CCKLR-17D3*^{Δ1}; $P = 0.6697$ for *CCKLR-17D3*^{Δ2}) on SD. Data represent means ± SEM ($n = 8$). n.s., not significant; * $P < 0.05$, ** $P < 0.01$, *** $P < 0.001$, as determined by Tukey's multiple comparisons test.

Figure 7—figure supplement 3. Transgenic silencing of *CCKLR-17D1* neurons suppresses injury-induced clustering in group-cultured male flies. Synaptic transmission in *CCKLR-17D1* neurons was blocked by transgenic expression of a tetanus toxin light chain (*17D1*>TNT). Heterozygous flies for Gal4 (*17D1*-Gal4/+) or TNT transgenes (TNT/+) served as negative controls. Two-way ANOVA detected significant interaction effects of genotype and injury (inj) on SD ($P = 0.0003$ for *17D1*-Gal4/+ vs. *17D1*>TNT; $P = 0.0012$ for TNT/+ vs. *17D1*>TNT). Data represent means ± SEM ($n = 8$). n.s., not significant; *** $P < 0.001$, as determined by Tukey's multiple comparisons test.

Figure 8. A working model for early-life social memory and the experience-dependent plasticity of SNB. Social distancing is an inheritable trait in *Drosophila*. Diverse genetic pathways contribute to active social preferences while the clustering property may have evolved to compensate for inferior traits in individuals and confer their group fitness. Nonetheless, *Drosophila* can tune their social distance depending on physiological states (e.g., mechanical injury) and this feature of SNB is defined as “social plasticity”. In fact, the social plasticity requires early-life social experience or “social memory” during development. Group culturing elevates DSK expression and DSK neuron activity to reinforce its postsynaptic signals likely to the cognate receptor *CCKLR-17D1*. The activation of DSK-*CCKLR-17D1* pathway thus encodes early-life social experience in developing brains to support social plasticity in adults.

Video 1. SNB in DGRP73 (grp + ctrl).

Video 2. SNB in DGRP360 (grp + ctrl).

Video 3. SNB in DGRP73 (large arena).

Video 4. SNB in DGRP360 (large arena).

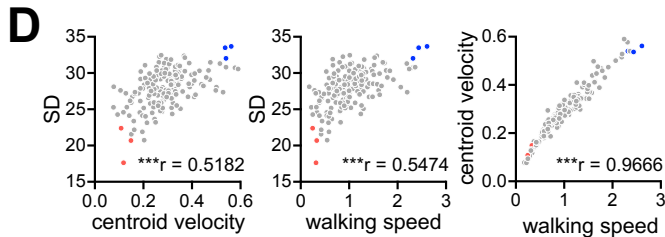
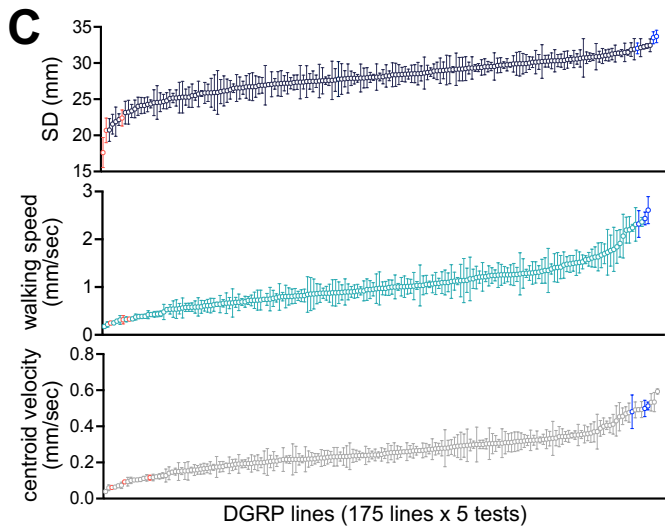
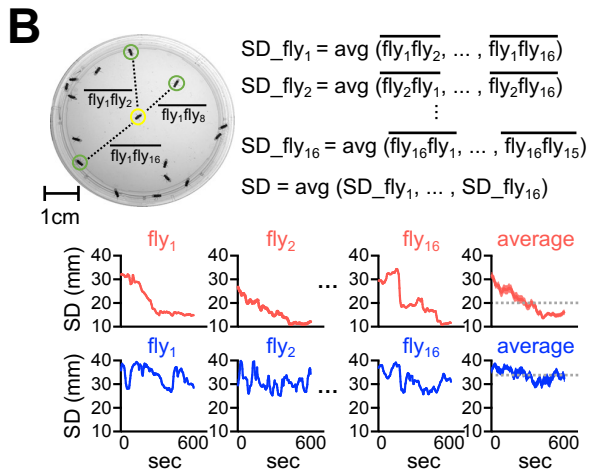
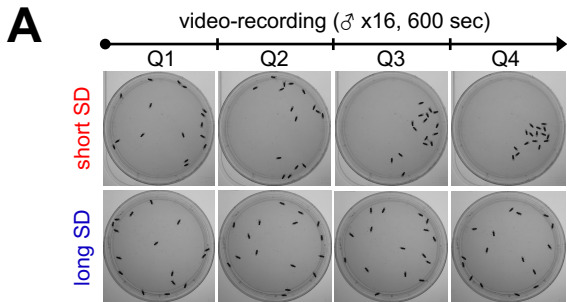
Video 5. SNB in DGRP73 (grp + inj).

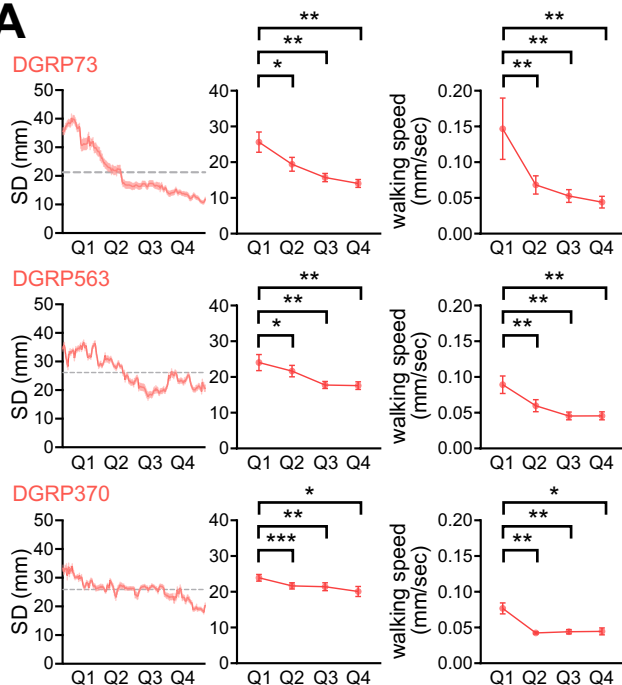
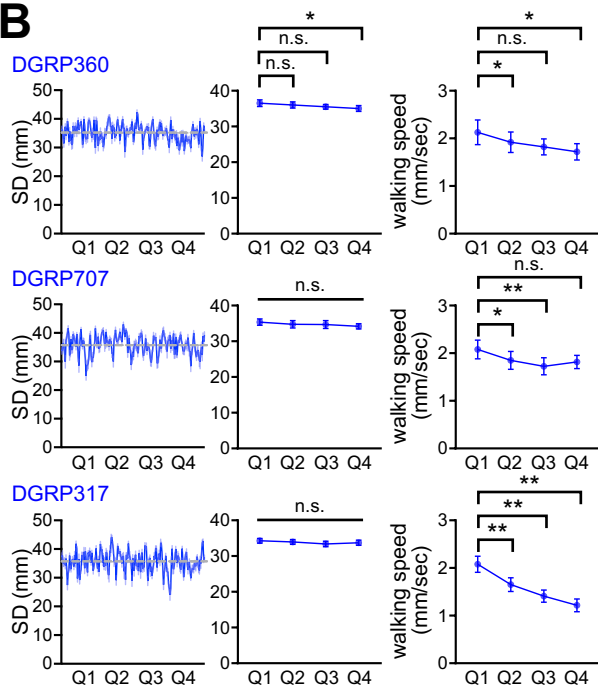
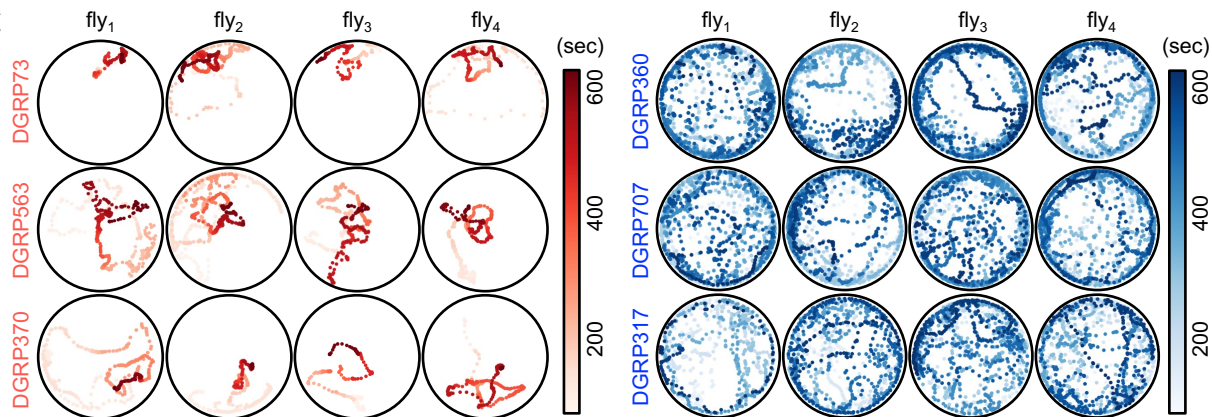
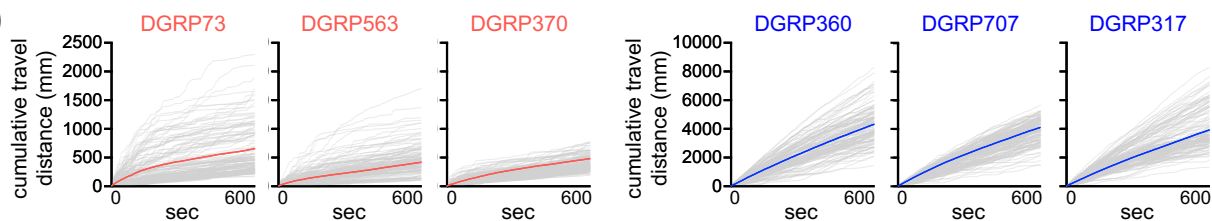
Video 6. SNB in DGRP360 (grp + inj).

Video 7. SNB in DGRP73 (iso + ctrl).

Video 8. SNB in DGRP360 (iso + ctrl).

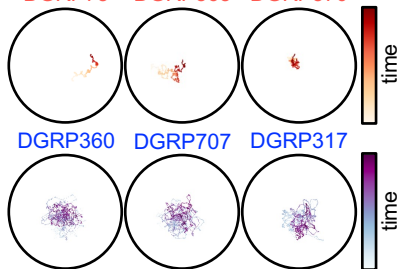
- 1113 **Video 9. SNB in DGRP73 (iso + inj).**
- 1114 **Video 10. SNB in DGRP360 (iso + inj).**
- 1115 **Video 11. Aggression behaviors in DGRP73.**
- 1116 **Video 12. Aggression behaviors in DGRP360.**



A**B****C****D**

centroid trajectories

DGRP73 DGRP563 DGRP370



DGRP360 DGRP707 DGRP317

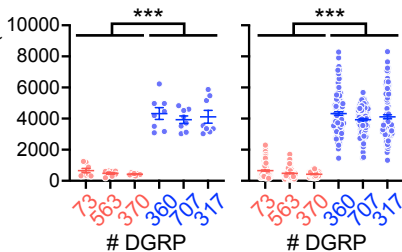
time

C

averaged
per experiment

individuals

travel distance (mm)



DGRP

DGRP

B

● grp ● iso

- grp
- iso

SD (mm)

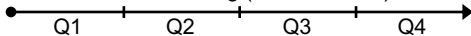
walking speed
(mm/sec)

centroid velocity
(mm/sec)

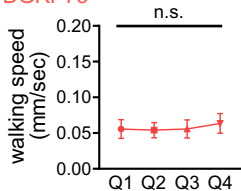
DGRP

DGRP

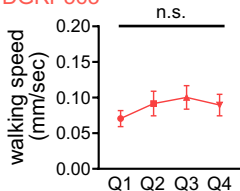
video-recording (δ x1, 600 sec)



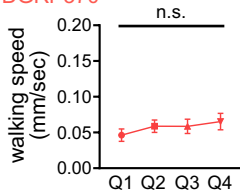
DGRP73



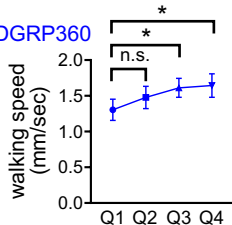
DGRP563



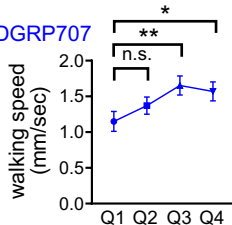
DGRP370



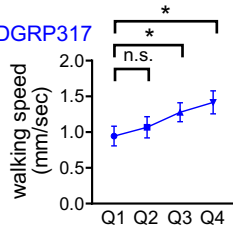
DGRP360



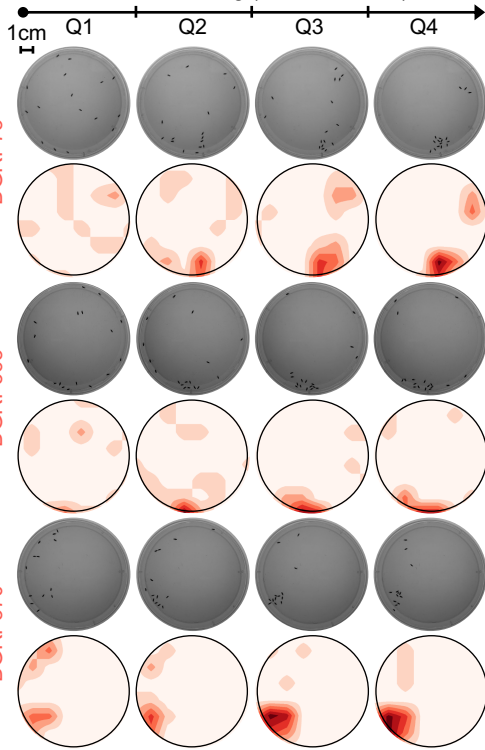
DGRP707



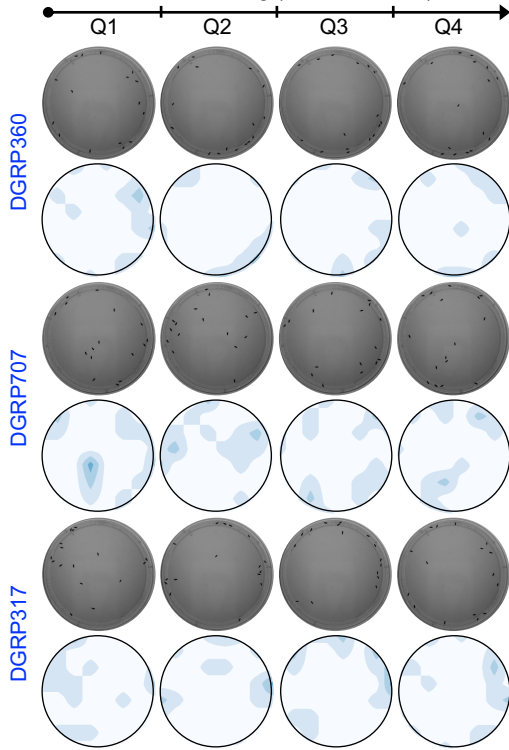
DGRP317

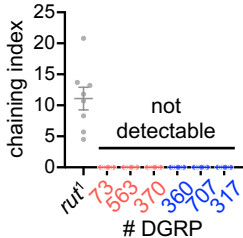


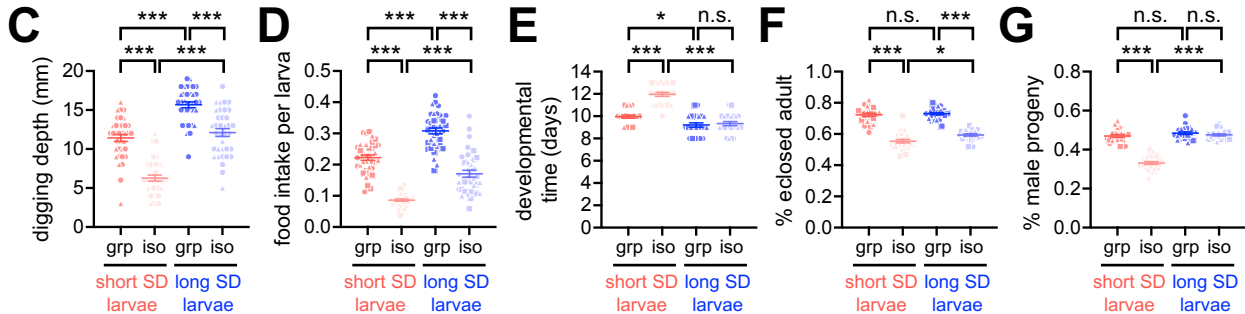
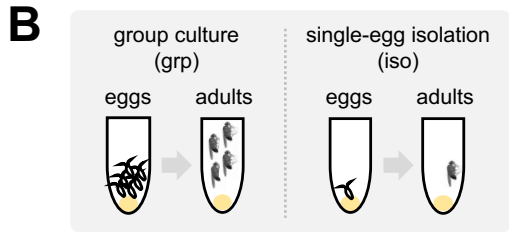
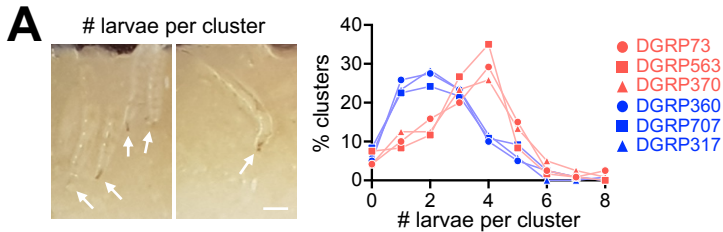
video-recording (σ x16, 600 sec)

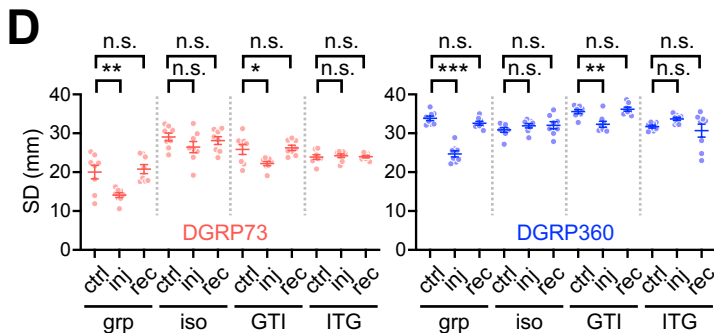
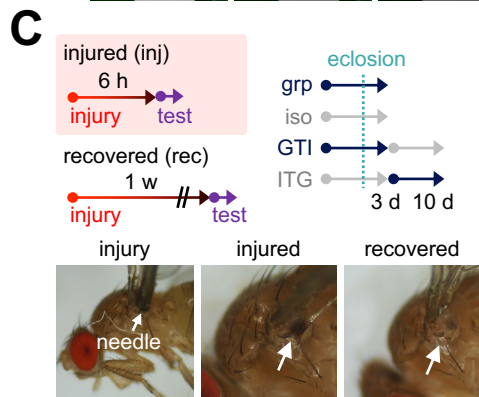
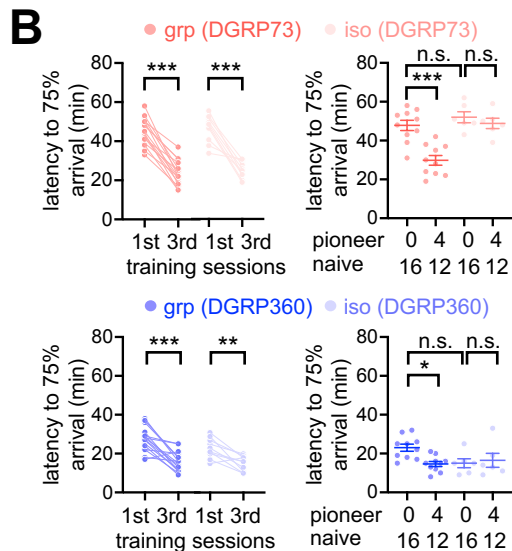
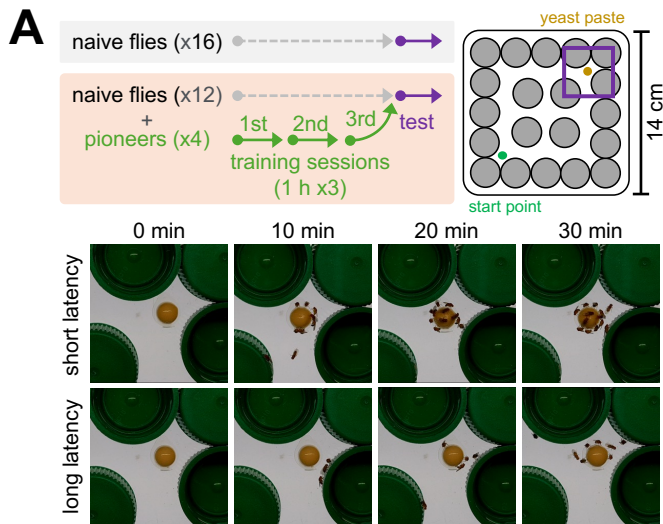


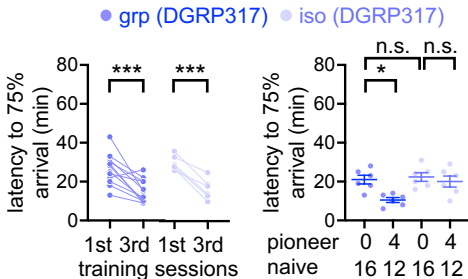
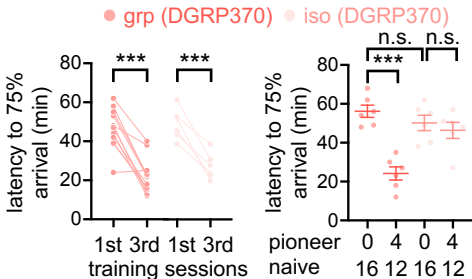
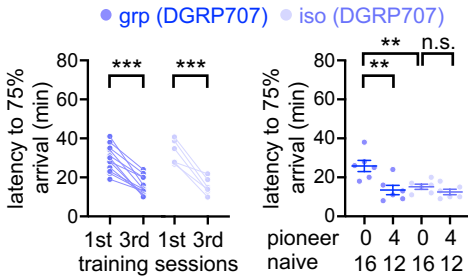
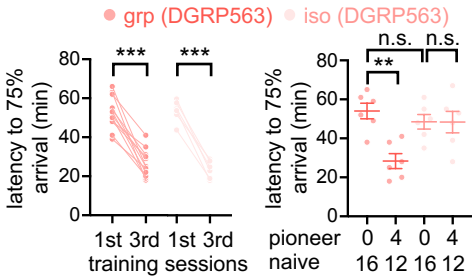
video-recording (σ x16, 600 sec)

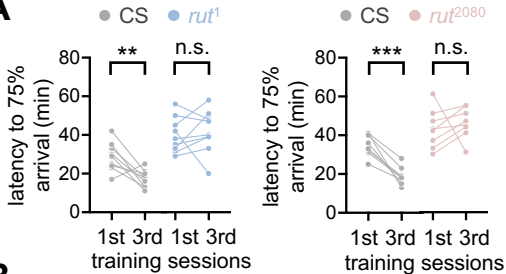
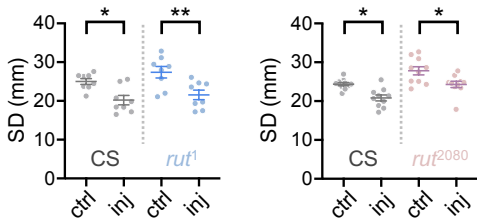


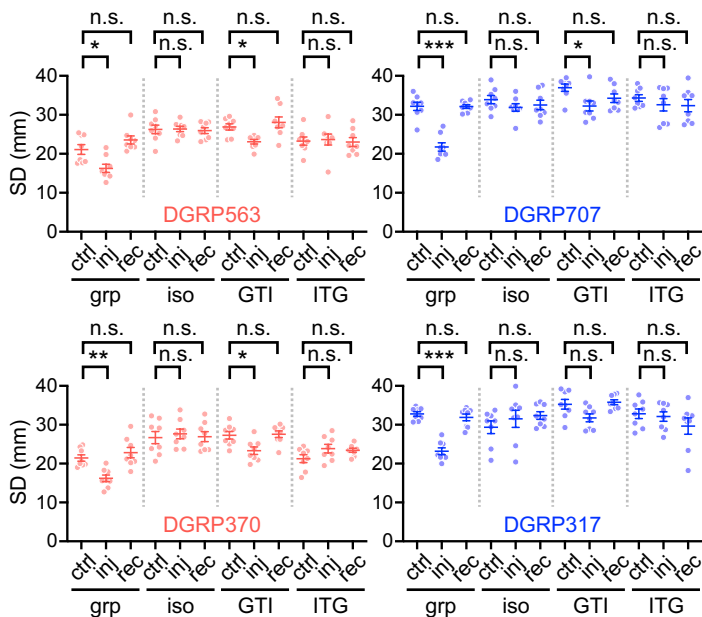
A*rut¹***B**



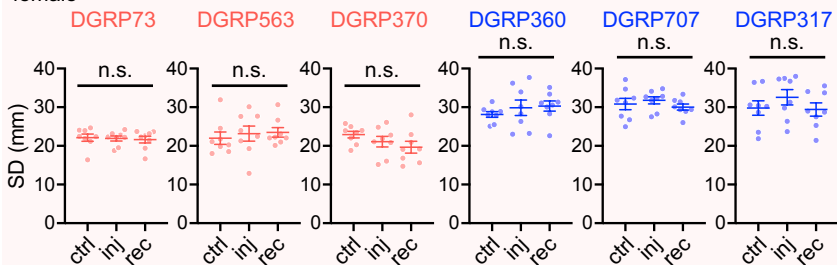


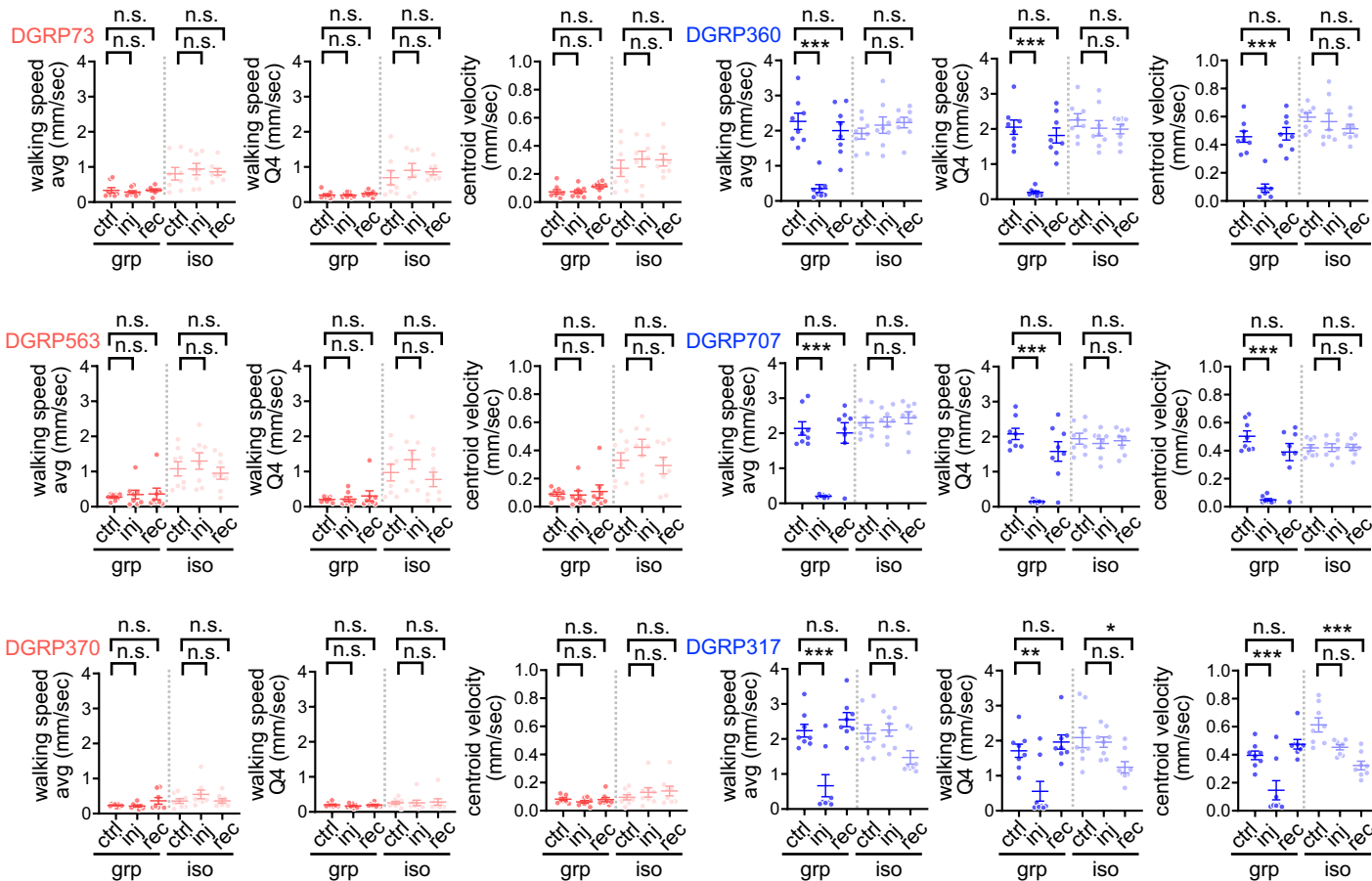


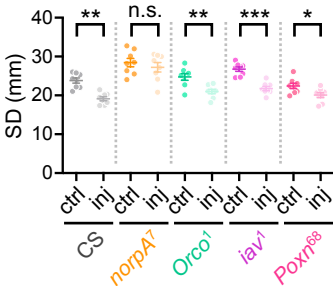
A**B**

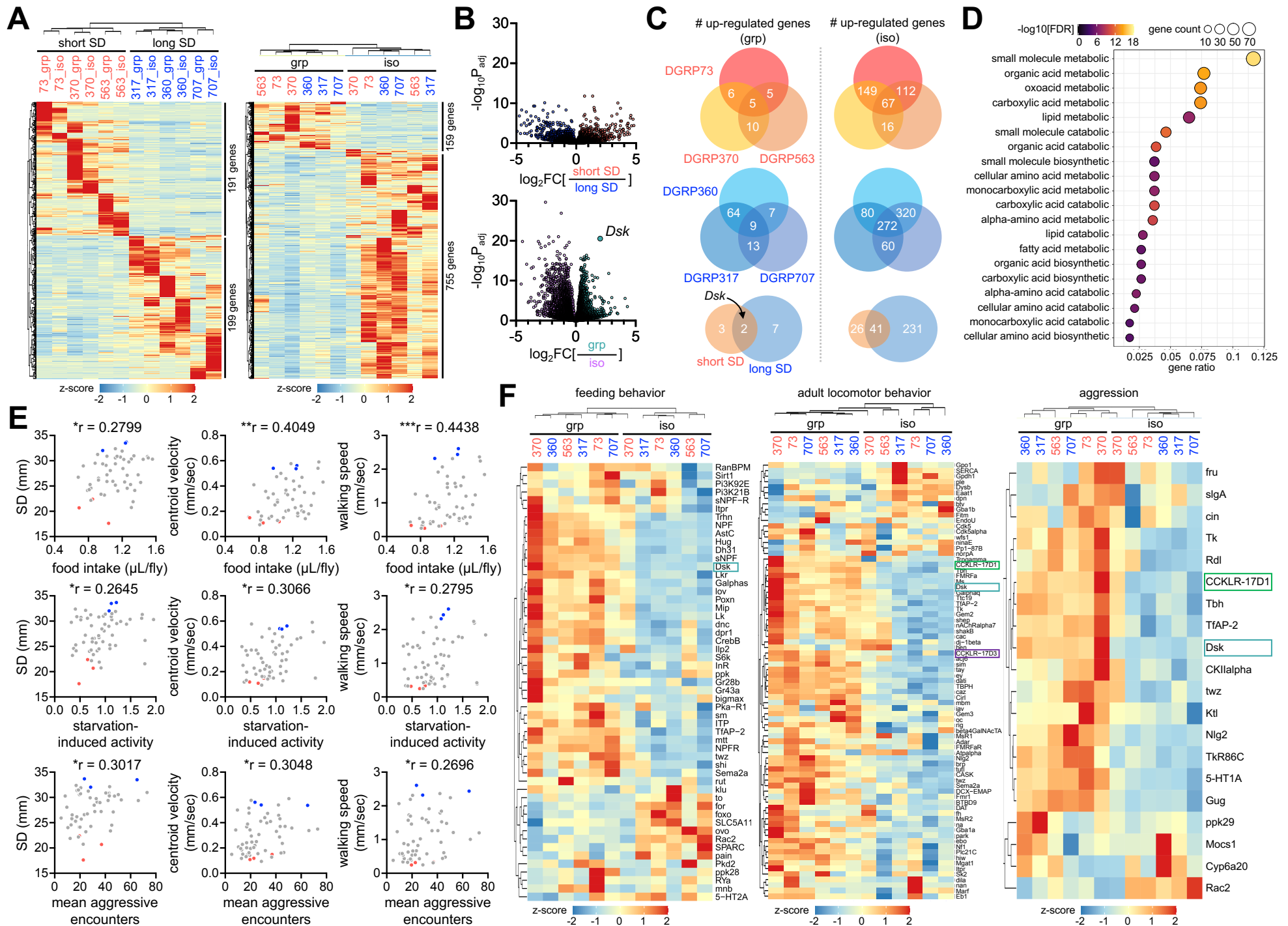
A**B**

female



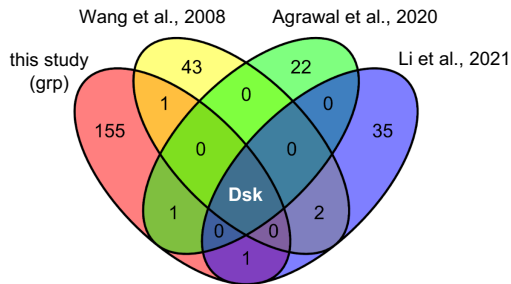




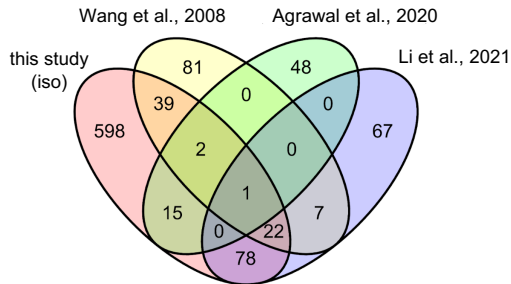


A

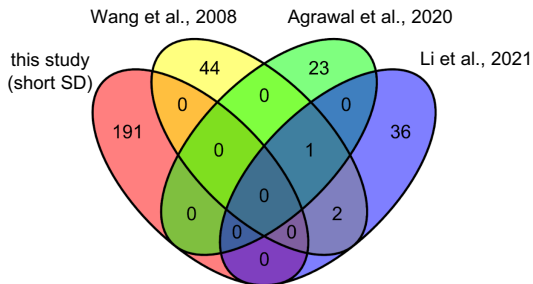
up-regulated genes (grp)



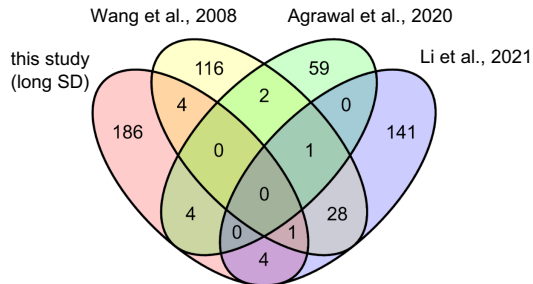
up-regulated genes (iso)

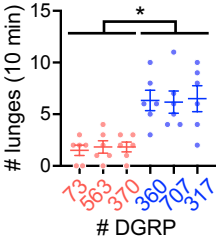
**B**

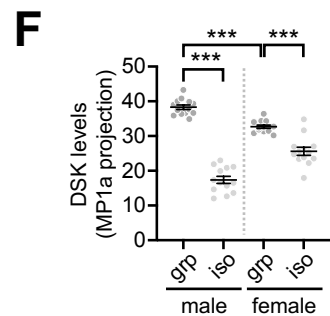
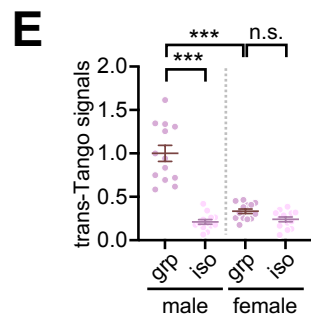
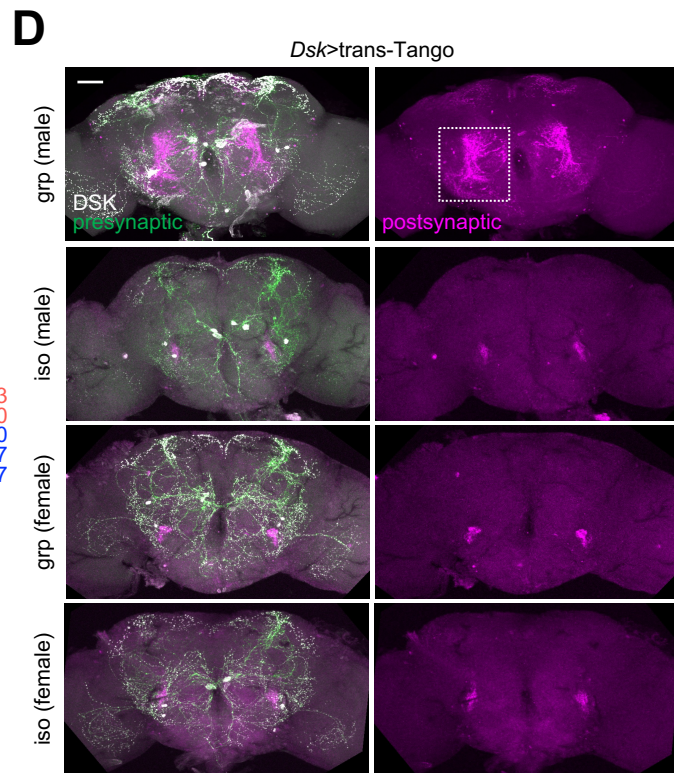
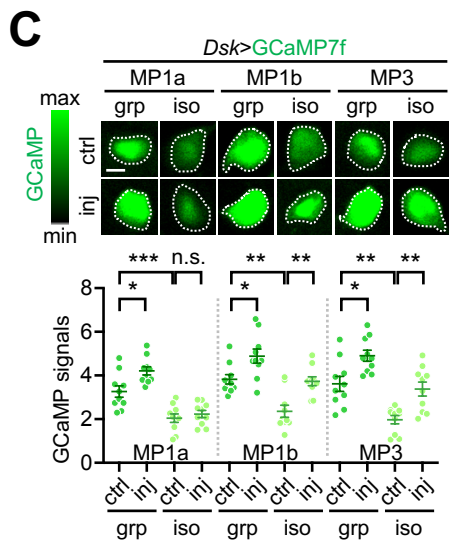
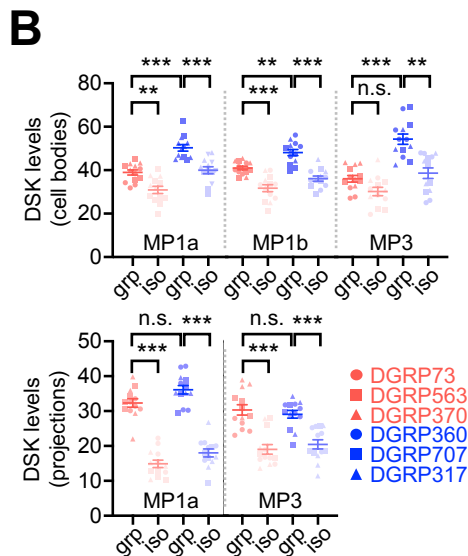
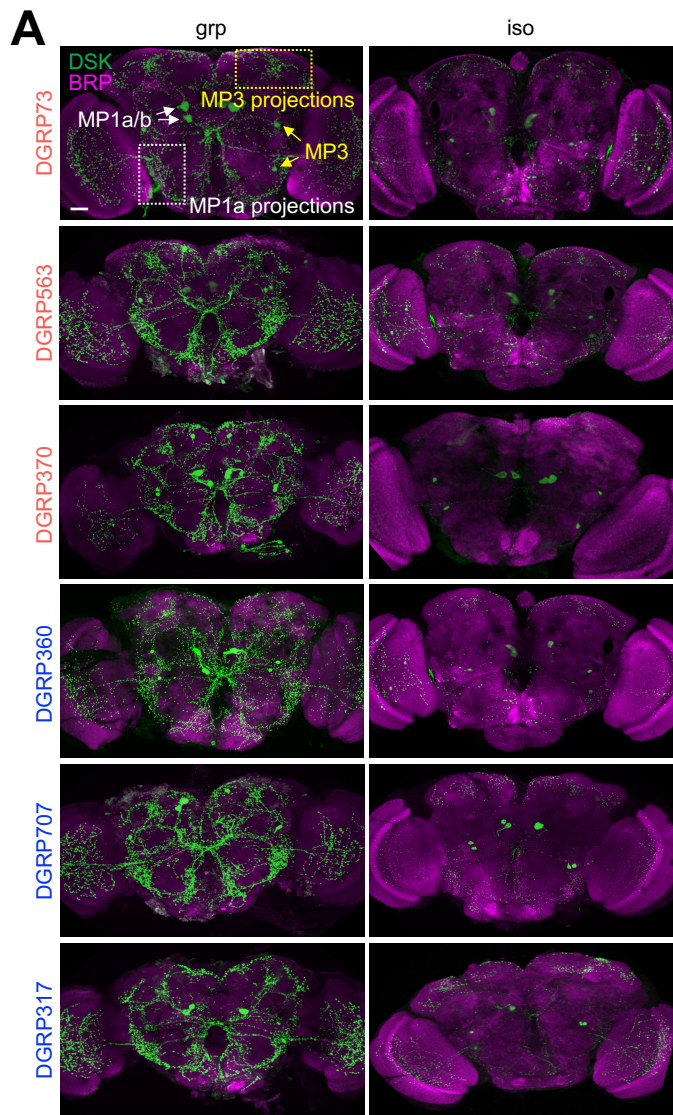
up-regulated genes (short SD vs. grp)

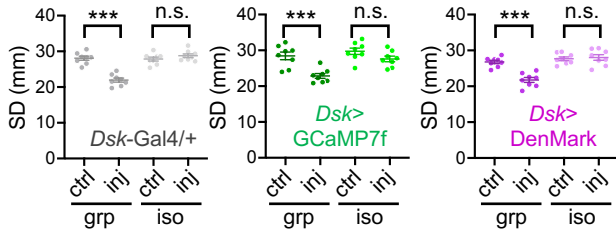
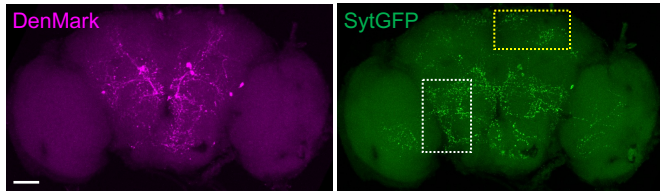
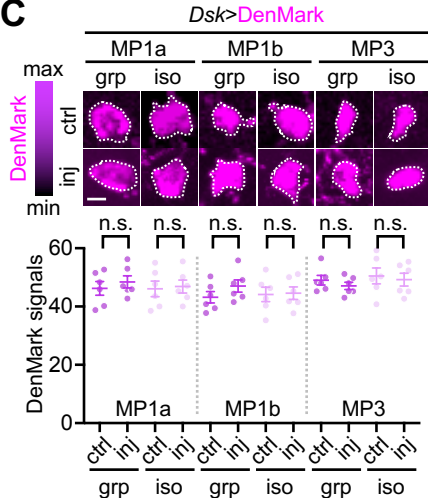


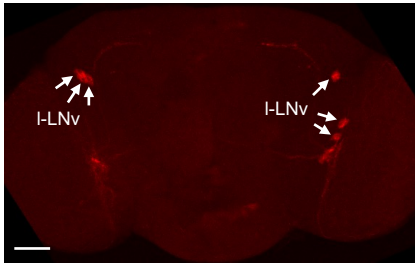
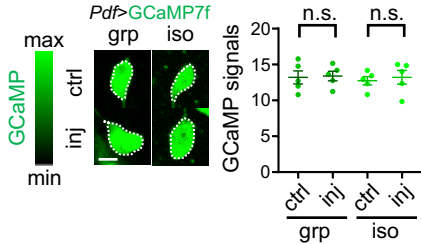
up-regulated genes (long SD vs. iso)

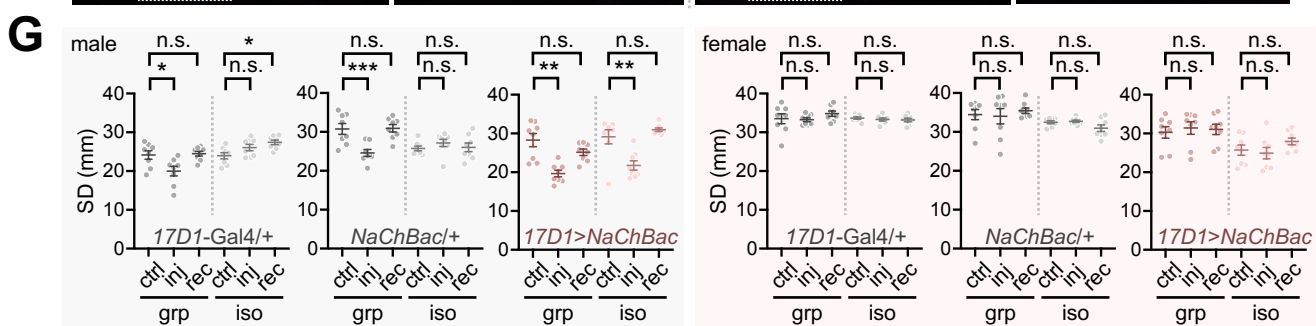
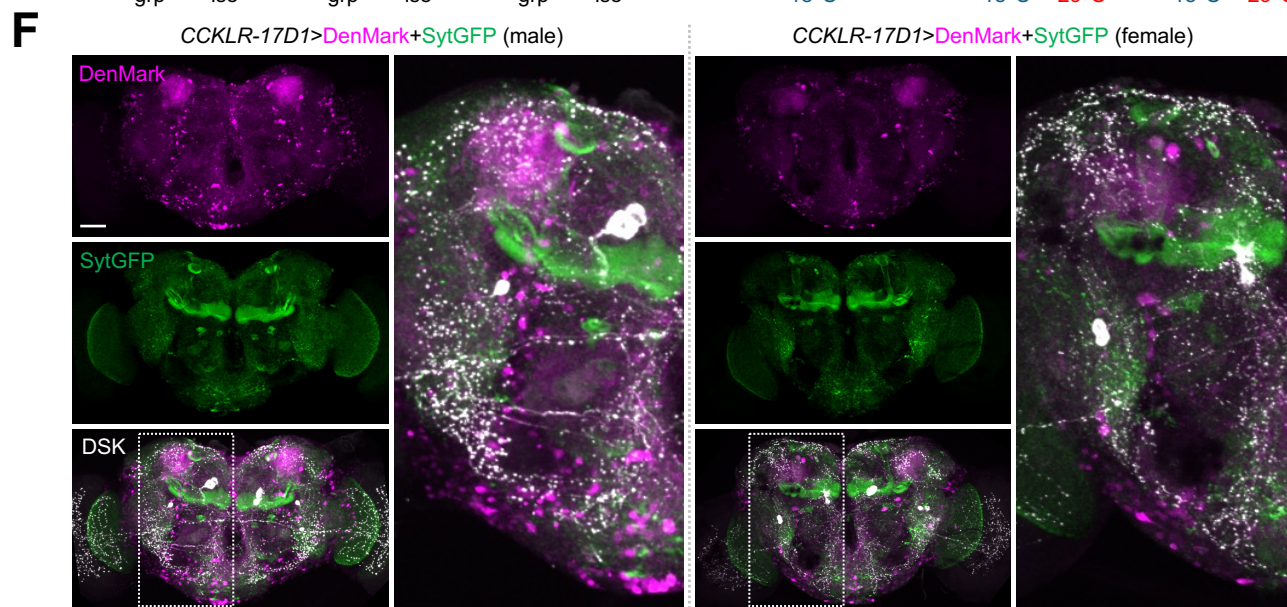
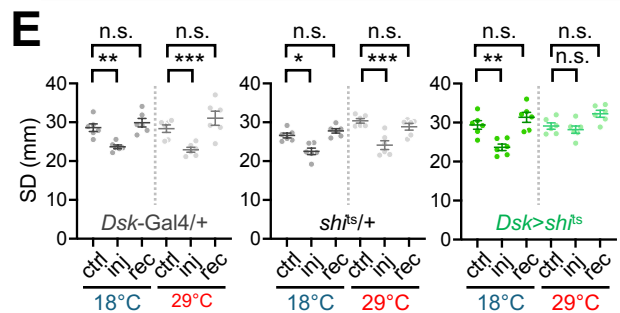
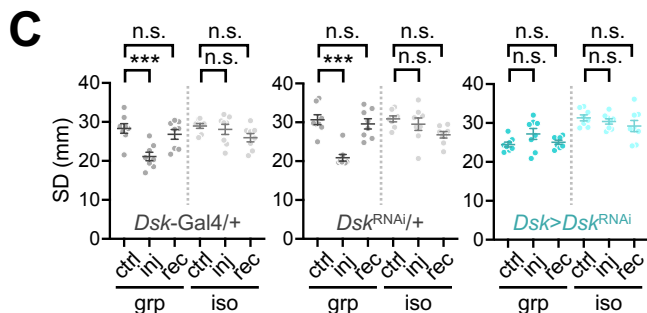
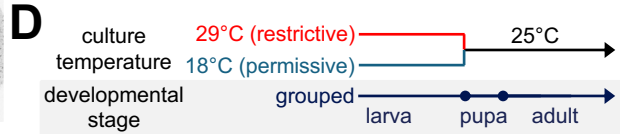
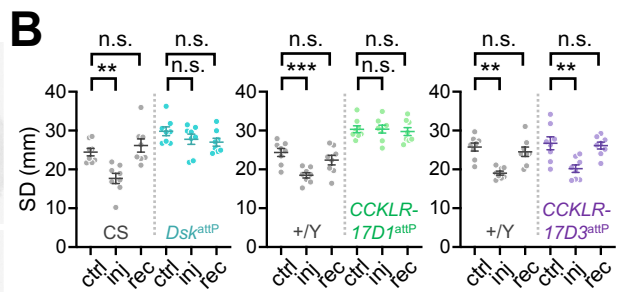
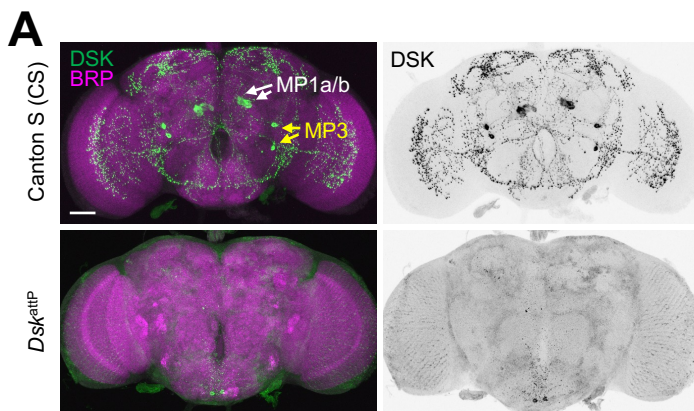




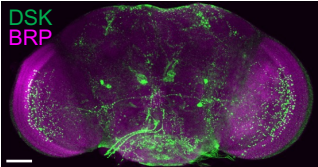


A**B***Dsk>DenMark* + *SytGFP***C**

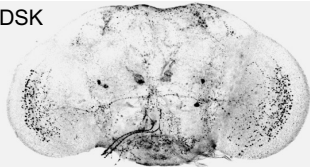
A*Pdf*>mRFP**B**



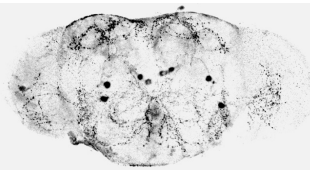
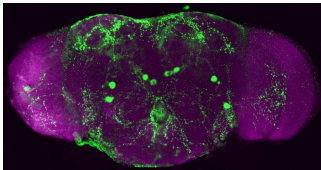
Dsk-Gal4/+



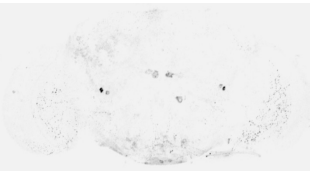
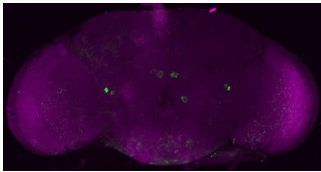
DSK

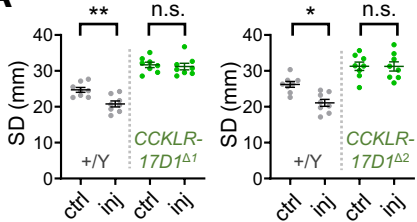
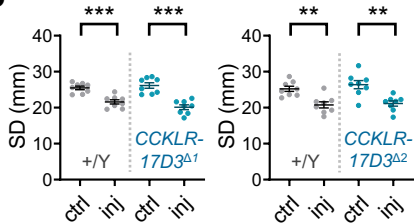


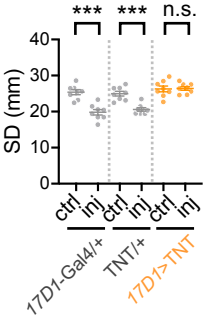
Dsk^{RNAi}/+



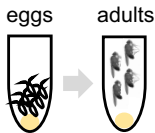
Dsk>Dsk^{RNAi}



A**B**

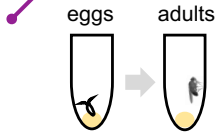


socially enriched
development



DSK-CCKLR-17D1
pathway

socially isolated
development



encoding early-life **social memory**

*physiological
challenge*



social plasticity



adaptive evolution with genetic diversity

inferior traits in
short-SD individuals

- hypoactive
- low food intake
- longer development
- low male progeny

*compensated by
group property*

superior traits in
long-SD individuals

- hyperactive
- high food intake
- high aggression